Chan, D.C., Fass, D., Berger, J.M., Kim, P.S., 1997. Core structure of gp41 from the HIV envelope glycoprotein. Cell 89, 263–273.
De Clercq, E., Yamamoto, N., Pauwels, R., Balzarini, J., Witvrouw, M., De Vreese, K., Debyser, Z., Rosenwirth, B., Peichl, P., Datema, R., et al., 1994. Highly potent and selective inhibition of human immunodeficiency virus by the bicyclam derivative JM3100. Antimicrob. Agents Chemother. 38, 668–674.
Dodt, J., Schmitz, T., Schäfer, T., Bergmann, C., 1986. Expression, secretion and processing of hirudin in *E. coli* using the alkaline phosphatase signal sequence. FEBS Lett. 202, 373–377.
Eckert, D.M., Kim, P.S., 2001. Mechanisms of viral membrane fusion and its inhibition. Annu. Rev. Biochem. 70, 777–810.
Fätkenheuer, G., Pozniak, A.L., Johnson, M.A., Plettenberg, A., Staszewski, S., Hoepelman, A.I., Saag, M.S., Goebel, F.D., Rockstroh, J.K., Dezube, B.J., Jenkins, T.M., Medhurst, C., Sullivan, J.F., Ridgway, C., Abel, S., James, I.T., Youle, M., van der Ryst, E., 2005. Efficacy of short-term monotherapy with maraviroc, a new CCR5 antagonist, in patients infected with HIV-1. Nat. Med. 11, 1170–1172.
Ferrer, M., Kapoor, T.M., Strassmaier, T., Weissenhorn, W., Skehel, J.J., Oprian, D., Schreiber, S.L., Wiley, D.C., Harrison, S.C., 1999. Selection of gp41-mediated HIV-1 cell entry inhibitors from biased combinatorial libraries of non-natural binding elements. Nat. Struct. Biol. 6, 953–960.
Frey, G., Rits-Volloch, S., Zhang, X.Q., Schooley, R.T., Chen, B., Harrison, S.C., 2006. Small molecules that bind the inner core of gp41 and inhibit HIV envelope-mediated fusion. Proc. Natl. Acad. Sci. U.S.A. 103, 13938–13943.
Grinsztejn, B., Nguyen, B.Y., Katlama, C., Gatell, J.M., Lazzarin, A., Vittecoq, D., Gonzalez, C.J., Chen, J., Harvey, C.M., Isaacs, R.D., 2007. Safety and efficacy of the HIV-1 integrase inhibitor raltegravir (MK-0518) in treatment-experienced patients with multidrug-resistant virus: a phase II randomised controlled trial. Lancet 369, 1261–1269.
Hazuda, D.J., Young, S.D., Guare, J.P., Anthony, N.J., Gomez, R.P., Wai, J.S., Vacca, J.P., Handt, L., Motzel, S.L., Klein, H.J., Dornadula, G., Danovich, R.M., Witmer, M.V., Wilson, K.A., Tussey, L., Schleif, W.A., Gabryelski, L.S., Jin, L., Miller, M.D., Casimiro, D.R., Emini, E.A., Shiver, J.W., 2004. Integrase inhibitors and cellular immunity suppress retroviral replication in rhesus macaques. Science 305, 528–532.
Huang, J.H., Liu, Z.Q., Liu, S., Jiang, S., Chen, Y.H., 2006. Identification of the HIV-1 gp41 core-binding motif—HXXNPF. FEBS Lett. 580, 4807–4814.
Huang, J.H., Yang, H.W., Liu, S., Li, J., Jiang, S., Chen, Y.H., 2007. The mechanism by which molecules containing the HIV gp41 core-binding motif HXXNPF inhibit HIV-1 envelope glycoprotein-mediated syncytium formation. Biochem. J. 403, 565–571.
Jahn, R., Lang, T., Südhof, T.C., 2003. Membrane fusion. Cell 112, 519–533.
Jiang, S., Lin, K., Zhang, L., Debnath, A.K., 1999. A screening assay for antiviral compounds targeted to the HIV-1 gp41 core structure using a conformation-specific monoclonal antibody. J. Virol. Methods 80, 85–96.
Kikuchi, Y., Yoda, K., Yamasaki, M., Tamura, G., 1981. The nucleotide sequence of the promoter and the amino-terminal region of alkaline phosphatase structural gene (phoA) of *Escherichia coli*. Nucl. Acids Res. 9, 5671–5678.
Kimpton, J., Emerman, M., 1992. Detection of replication-competent and pseudotyped human immunodeficiency virus with a sensitive cell line on the basis of activation of an integrated beta-galactosidase gene. J. Virol. 66, 2232–2239.
Kobe, B., Center, R.J., Kemp, B.E., Poumbourios, P., 1999. Crystal structure of human T cell leukemia virus type 1 gp21 ectodomain crystallized as a maltose-binding protein chimera reveals structural evolution of retroviral transmembrane proteins. Proc. Natl. Acad. Sci. U.S.A. 96, 4319–4324.
Kodama, E.I., Kohgo, S., Kitano, K., Machida, H., Gatanaga, H., Shigeta, S., Matsuoka, M., Ohrui, H., Mitsuya, H., 2001. 4′-Ethynyl nucleoside analogs: potent inhibitors of multidrug-resistant human immunodeficiency virus variants in vitro. Antimicrob. Agents Chemother. 45, 1539–1546.
Lalezari, J.P., Henry, K., O'Hearn, M., Montaner, J.S., Piliero, P.J., Trottier, B., Walmsley, S., Cohen, C., Kuritzkes, D.R., Eron Jr., J.J., Chung, J., DeMasi, R., Donatacci, L., Drobnes, C., Delehanty, J., Salgo, M., 2003. Enfuvirtide, an HIV-1 fusion inhibitor, for drug-resistant HIV infection in North and South America. N. Engl. J. Med. 348, 2175–2185.
Lazzarin, A., Clotet, B., Cooper, D., Reynes, J., Arasteh, K., Nelson, M., Katlama, C., Stellbrink, H.J., Delfraissy, J.F., Lange, J., Huson, L., DeMasi, R., Wat, C., Delehanty, J., Drobnes, C., Salgo, M., 2003. Efficacy of enfuvirtide in patients infected with drug-resistant HIV-1 in Europe and Australia. N. Engl. J. Med. 348, 2186–2195.
Liu, S., Jing, W., Cheung, B., Lu, H., Sun, J., Yan, X., Niu, J., Farmar, J., Wu, S., Jiang, S., 2007. HIV gp41 C-terminal heptad repeat contains multifunctional domains. Relation to mechanisms of action of anti-HIV peptides. J. Biol. Chem. 282, 9612–9620.
Liu, S., Lu, H., Niu, J., Xu, Y., Wu, S., Jiang, S., 2005. Different from the HIV fusion inhibitor C34, the anti-HIV drug Fuzeon (T-20) inhibits HIV-1 entry by targeting multiple sites in gp41 and gp120. J. Biol. Chem. 280, 11259–11273.
Medinas, R.J., Lambert, D.M., Tompkins, W.A., 2002. C-terminal gp40 peptide analogs inhibit feline immunodeficiency virus: cell fusion and virus spread. J. Virol. 76, 9079–9086.
Mink, M., Mosier, S.M., Janumpalli, S., Davison, D., Jin, L., Melby, T., Sista, P., Erickson, J., Lambert, D., Stanfield-Oakley, S.A., Salgo, M., Cammack, N., Matthews, T., Greenberg, M.L., 2005. Impact of human immunodeficiency virus type 1 gp41 amino acid substitutions selected during enfuvirtide treatment on gp41 binding and antiviral potency of enfuvirtide in vitro. J. Virol. 79, 12447–12454.
Nameki, D., Kodama, E., Ikeuchi, M., Mabuchi, N., Otaka, A., Tamamura, H., Ohno, M., Fujii, N., Matsuoka, M., 2005. Mutations conferring resistance to human immunodeficiency virus type 1 fusion inhibitors are restricted by gp41 and Rev-responsive element functions. J. Virol. 79, 764–770.
Otaka, A., Nakamura, M., Nameki, D., Kodama, E., Uchiyama, S., Nakamura, S., Nakano, H., Tamamura, H., Kobayashi, Y., Matsuoka, M., Fujii, N., 2002. Remodeling of gp41-C34 peptide leads to highly effective inhibitors of the fusion of HIV-1 with target cells. Angew. Chem. Int. Ed. Engl. 41, 2937–2940.
Poveda, E., Rodés, B., Toro, C., Martín-Carbonero, L., Gonzalez-Lahoz, J., Soriano, V., 2002. Evolution of the gp41 env region in HIV-infected patients receiving T-20, a fusion inhibitor. AIDS 16, 1959–1961.
Rimsky, L.T., Shugars, D.C., Matthews, T.J., 1998. Determinants of human immunodeficiency virus type 1 resistance to gp41-derived inhibitory peptides. J. Virol. 72, 986–993.
Root, M.J., Kay, M.S., Kim, P.S., 2001. Protein design of an HIV-1 entry inhibitor. Science 291, 884–888.
Ryu, J.R., Lee, J., Choo, S., Yoon, S.H., Woo, E.R., Yu, Y.G., 1998. Development of an in vitro assay system for screening of gp41 inhibitory compounds. Mol. Cells 8, 717–723.
Schibli, D.J., Weissenhorn, W., 2004. Class I and class II viral fusion protein structures reveal similar principles in membrane fusion. Mol. Membr. Biol. 21, 361–371.
Tagat, J.R., McCombie, S.W., Nazareno, D., Labroli, M.A., Xiao, Y., Steensma, R.W., Strizki, J.M., Baroudy, B.M., Cox, K., Lachowicz, J., Varty, G., Watkins, R., 2004. Piperazine-based CCR5 antagonists as HIV-1 inhibitors. IV. Discovery of 1-[(4,6-dimethyl-5-pyrimidinyl)carbonyl]-4-[4-[2-methoxy-1(*R*)-4-(trifluoromethyl)phenyl]ethyl-3(*S*)-methyl-1-piperazinyl]-4-methylpiperidine (Sch-417690/Sch-D), a potent, highly selective, and orally bioavailable CCR5 antagonist. J. Med. Chem. 47, 2405–2408.
Watanabe, S., Takada, A., Watanabe, T., Ito, H., Kida, H., Kawaoka, Y., 2000. Functional importance of the coiled-coil of the Ebola virus glycoprotein. J. Virol. 74, 10194–10201.
Wei, X., Decker, J.M., Liu, H., Zhang, Z., Arani, R.B., Kilby, J.M., Saag, M.S., Wu, X., Shaw, G.M., Kappes, J.C., 2002. Emergence of resistant human immunodeficiency virus type 1 in patients receiving fusion inhibitor (T-20) monotherapy. Antimicrob. Agents Chemother. 46, 1896–1905.
Wexler-Cohen, Y., Shai, Y., 2007. Demonstrating the C-terminal boundary of the HIV 1 fusion conformation in a dynamic ongoing fusion process and implication for fusion inhibition. FASEB J. 21, 3677–3684.
Xu, Y., Hixon, M.S., Dawson, P.E., Janda, K.D., 2007. Development of a FRET assay for monitoring of HIV gp41 core disruption. J. Org. Chem. 72, 6700–6707.

Bioorganic & Medicinal Chemistry Letters 18 (2008) 4124–4129

Contents lists available at ScienceDirect

Bioorganic & Medicinal Chemistry Letters

journal homepage: www.elsevier.com/locate/bmcl

Identification of novel non-peptide CXCR4 antagonists by ligand-based design approach

Satoshi Ueda [a], Manabu Kato [a], Shinsuke Inuki [a], Hiroaki Ohno [a], Barry Evans [b], Zi-xuan Wang [b], Stephen C. Peiper [b], Kazuki Izumi [c], Eiichi Kodama [c], Masao Matsuoka [c], Hideko Nagasawa [d], Shinya Oishi [a,*], Nobutaka Fujii [a,*]

[a] Graduate School of Pharmaceutical Sciences, Kyoto University, Sakyo-ku, Kyoto 606-8501, Japan
[b] Department of Pathology, Medical College of Georgia, GA 30912, USA
[c] Institute for Virus Research, Kyoto University, Sakyo-ku, Kyoto 606-8507, Japan
[d] Gifu Pharmaceutical University, Mitahora-higashi, Gifu 502-8585, Japan

ARTICLE INFO

Article history:
Received 6 April 2008
Revised 21 May 2008
Accepted 22 May 2008
Available online 29 May 2008

Keywords:
Chemokine
CXCR4
SDF-1
Anti-HIV
Indole

ABSTRACT

The design and synthesis of novel non-peptide CXCR4 antagonists is described. The peptide backbone of highly potent cyclic peptide-based CXCR4 antagonists was entirely replaced by an indole framework, which was expected to reproduce the disposition of the key pharmacophores consistent with those of potential bioactive conformations of the original peptides. A structure–activity relationship study on a series of modified indoles identified novel small-molecule antagonists having three pharmacophore functional groups through the appropriate linkers.

Chemokines are a family of small proteins with chemotactic and proactivatory effects on leukocytes. Chemokines mediate their biological effects by binding to the specific G-protein coupled receptor subtypes that are differentially and widely expressed in blood cells. Among these chemokine receptors, CXCR4 has a broad tissue distribution and the activation by its endogenous ligand CXCL12 (SDF-1, stromal cell-derived factor 1) leads to chemotaxis, immunomodulation, and other regulatory functions including progenitor cell migration during embryologic development of the cardiovascular, hematopoietic, and central nervous systems. In addition to its physiological roles, CXCR4 also plays important roles in pathological conditions. These include tumor growth and metastasis[1] and rheumatoid arthritis (RA).[2] CXCR4 has also been reported to act as a major co-receptor involved in the entry of T-cell-line-tropic human immunodeficiency virus type 1 (HIV-1) strains into target cells.[3] Thus, CXCR4 is considered as an important therapeutic target for multiple diseases. Inhibitory compounds of CXCL12 or HIV-1 binding to CXCR4 could be novel classes of anti-cancer, anti-RA, and anti-HIV-1 drugs. Previously, we found highly potent peptide-based CXCR4 antagonists such as **1**, **2**, and **3** (Fig. 1).[4,5]

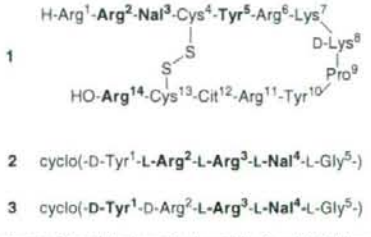

Figure 1. Structures of **1** and its downsized peptides **2** and **3**. Bold residues are the indispensable residues for the potent CXCR4-antagonistic activity. Nal, L-3-(2-naphthyl)alanine; Cit, L-citrulline.

Peptide **1** and its derivatives effectively blocked X4-HIV-1 entry to the cell by specifically binding to CXCR4,[6] and also showed an anti-metastatic effect against breast cancer[7] and anti-RA activity[8] in mouse models.

Although peptides are excellent lead molecules for development of pharmaceutical agents, special drug delivery systems are usually required for their clinical use because of the poor bioavailability and instability against enzymes. Whereas several peptide-based CXCR4 antagonists have been reported, only small numbers of small-molecule CXCR4 antagonists have been

* Corresponding authors. Tel: +81 75 753 4551; fax: +81 75 753 4570 (N. Fujii).
E-mail addresses: soishi@pharm.kyoto-u.ac.jp (S. Oishi), nfujii@pharm.kyoto-u.ac.jp (N. Fujii).

0960-894X/$ - see front matter © 2008 Elsevier Ltd. All rights reserved.
doi:10.1016/j.bmcl.2008.05.092

reported.[9] These prompted us to design novel non-peptide CXCR4 antagonists based on the SAR and conformational studies on peptide ligands **1**–**3**.

Cyclic pentapeptide-based CXCR4 antagonists **2** and **3** were identified by screening of cyclic pentapeptide libraries, which were designed based on SAR studies of peptide **1**. The constrained backbone of the cyclic peptide was utilized as a template for positioning the key functional groups in space as is found in parent peptide **1**. Subsequent conformational analysis of **2** permitted us to determine the topology of the four indispensable residues, then, rational approach toward the de novo design of non-peptide antagonists may be envisaged.[10]

Our previous SAR studies on **2** and its derivatives have shown that at least three functional groups on the peptide side-chains are required: (1) an aromatic ring such as 2-naphthyl- or 3-indolyl group at position 4; (2) a guanidino group at position 3; (3) a guanidino group at position 2 or a phenol group at position 1.[11] However, it was difficult to determine the spatial relationships between these functional groups due to the free rotation of the side-chain torsion (χ) angles. In our structural analyses, peptide **2** adopted a

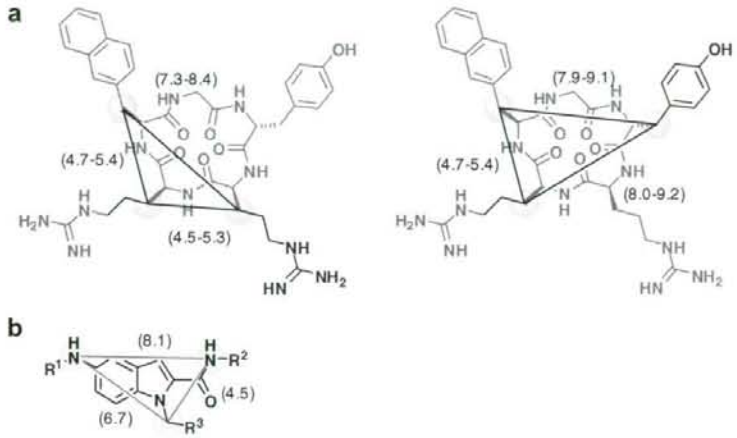

Figure 2. Design of indole-based CXCR4 antagonists based on molecular dynamics calculation of **2**. Distances (Å) between Cβ atoms bearing three essential functional groups during 1000 ps MD calculation of **2** (a) and between two key atoms of energy-minimized 5-acetamido-1-methylindole-2-carboxamide (b) are shown in parentheses. R^1–R^3 include naphthyl, indolyl, guanidino, and phenol groups.

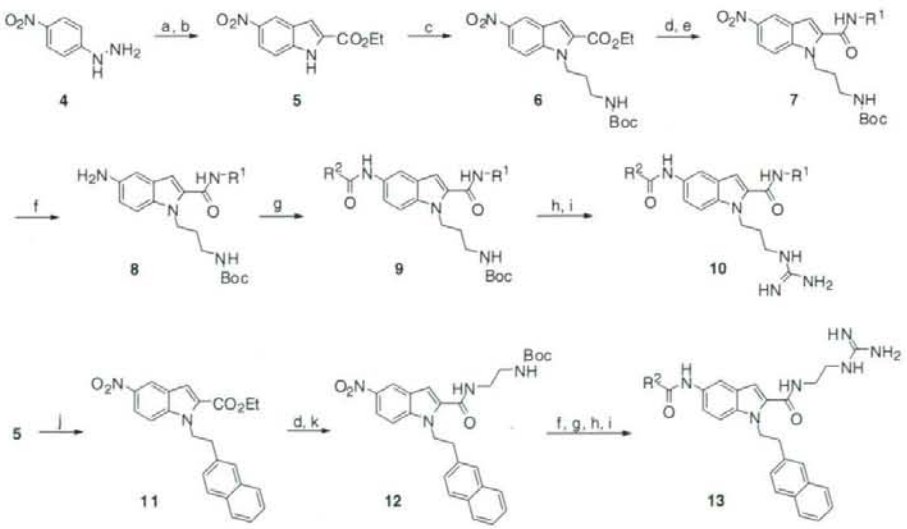

Scheme 1. Reagents and conditions: (a) ethyl pyruvate, EtOH, reflux; (b) polyphosphoric acid, xylene, 130 °C; (c) NaH, *N*-Boc-3-bromopropylamine, DMF, 70 °C; (d) 1 N NaOH aq., EtOH-THF; (e) R^1-NH_2, HATU, Et_3N, DMF; (f) NH_4CO_2H, Pd/C, EtOH-THF, reflux; (g) R^2-CO_2H, HATU, Et_3N, DMF; (h) 95% TFA-H_2O; (i) 1-*H*-pyrazolecarboxamidine hydrochloride, Et_3N, DMF; (j) 2-(2-naphthyl)ethyl bromide, NaH, DMF, 70 °C; (k) *N*-Boc-ethylenediamine, HATU, Et_3N, DMF.

variety of global conformations, in which the distances between indispensable functional groups were variable. On the other hand, relatively rigid cyclic peptide backbone and fixed distances between Cβ atoms, which append key functional groups, were observed.[5] Hence, we envisioned that introduction of crucial functional moieties for receptor binding onto a bicyclic heterocycle scaffold, which mimics the relatively fixed cyclic pentapeptide backbone of **2**, would provide non-peptide CXCR4 ligands. In this letter, we report a part of our ongoing research to develop novel non-peptide small molecule CXCR4 antagonists.

Among several molecular scaffold candidates, we first selected 5-aminoindole-2-carboxylic acid for the following reasons: (1) molecular modeling suggested that it met the spatial requirements for displaying the three key substituents (Fig. 2);[12] (2) accessible synthetic approaches were available for attachment of the three substituents; (3) indoles represent an important class of bioactive compounds and the physicochemical properties in terms of medicinal chemistry are well-documented.

Syntheses of indole-based compounds were achieved as shown in Scheme 1. (4-Nitrophenyl)hydrazine **4** was converted to the corresponding hydrazone, which was subjected to Fischer ring closure reaction to produce an indole **5**. Alkylation of N^1 position of the indole **5** with *N*-Boc-3-bromopropylamine gave **6**. This was hydrolyzed using 1 N aqueous sodium

Table 1
Inhibitory activities of indole derivatives **10a–j** and **13a–b** against binding of ^{125}I-SDF-1α to CXCR4

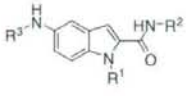

Compound	R^1	R^2	R^3	% inhibition at 10 μM
10a	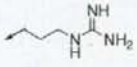	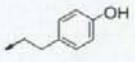	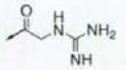	23
10b	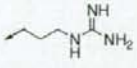	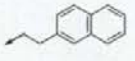	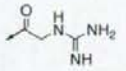	63
10c	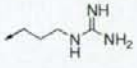	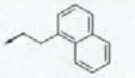	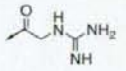	61
10d	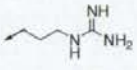	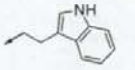	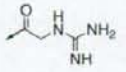	88
10e	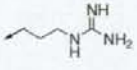	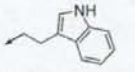	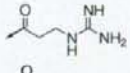	70
10f	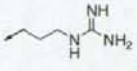	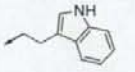	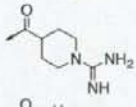	86
10g[a]	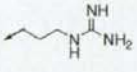	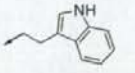	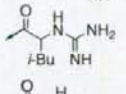	77
10h[a]	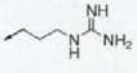	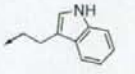	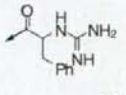	72
10i	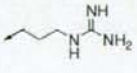		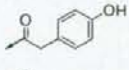	62
10j	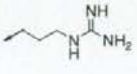		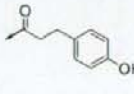	55
13a	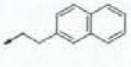	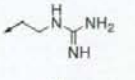	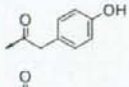	51
13b	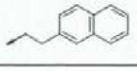	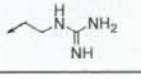	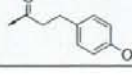	53

[a] Evaluated as a racemic mixture.

hydroxide in EtOH-THF and the resulting free carboxylic acid was coupled with amines using *O*-(7-azabenzotriazol-1-yl)-1,1,3,3-tetramethyluronium hexafluorophosphate (HATU) as coupling reagent to give **7**. The nitro group of **7** was reduced to amine **8** upon treatment with Pd-C and ammonium formate in EtOH. The aminoindole **8** was then coupled with carboxylic acids to give **9**. Deprotection of Boc group(s) by 95% TFA and guanylation of the free amino group(s) produced the target compounds **10**. Another series of compounds **13** were synthesized from **5** using similar reaction sequences described for **10**.

All indole-based compounds listed in Tables 1 and 2 were purified by preparative reverse-phase HPLC (purity >95%) and characterized by MALDI-TOF-MS. These compounds were tested for competitive binding inhibition in human CXCR4 transfected Chinese hamster ovary (CHO) cells using [^{125}I]SDF-1 as a radioligand, with the results given as percentage inhibition at 10 μM. IC_{50} values of selected compounds are shown in Table 2.

Compound **10d** with 2-(3-indolyl)ethyl group at the R^2 position showed 88% inhibition at 10 μM (IC_{50} = 3.0 μM) and was more potent than compounds having (4-hydroxyphenyl)-, (1-naphthyl)- or (2-naphthyl)-alkyl group at the R^2 position (compounds **10a–c**, 23–63% inhibition at 10 μM). Further SAR studies based on **10d** were undertaken. Chain elongation of the guanidinoacetyl group (R^3) of **10d** caused slight decrease in the affinity (**10e**). The use of *N*-amidinopiperidine-4-carbonyl was also acceptable for high potency [IC_{50} (**10f**) = 3.0 μM]. Introduction of an isobutyl or benzyl group into the α-carbon of guanidinomethyl carbonyl group of **10d** did not cause significant drop in binding affinity (compounds **10g** and **10h**). Compounds with *S*-configuration at the chiral center showed more potent CXCR4 antagonistic activity as compared with the corresponding *R*-isomers. (***S***)-**10g** was identified as the most potent compound [IC_{50} ((***S***)-**10g**) = 1.2 μM].[13] Compound (***S***)-**10g** also showed potent anti-HIV-1 activity (IIIB strain, inhibition of HIV-1 induced cytopathogenicity: EC_{50} = 5.4 μM). The IC_{50} value of (***S***)-**10g** is 34-fold lower as compared with parent peptide **2**. This is probably due to the absence of phenol functionality in (***S***)-**10g** which corresponds to D-Tyr side-chain of peptide **2**. Decreased number of amide bond in (***S***)-**10g** might also lead to the lower affinity. We have previously showed the importance of backbone amide functionalities of **2** for CXCR4 antagonistic activity by using reduced-amide isosteres or (*E*)-alkene dipeptide isosteres.[14]

Indole-based compounds having a phenol group at R^3 position showed moderate CXCR4-binding affinity (**10i**, **10j**, **13a**, and **13b**). Interestingly, these compounds did not show complete inhibition even at higher concentrations in the binding inhibition experiments, while compounds having a guanidino group at R^3 position (**10c**, **10d**, and (***S***)-**10g**) achieved complete inhibition (Fig. 3). These results suggest that **10c**, **10d** and (***S***)-**10g** are inhibitors that competitively bind to the SDF-1 binding site of CXCR4, while **10i**, **10j**, **13a**, and **13b** may bind to an allosteric site of CXCR4 and partially antagonize the SDF-1 binding.

Comparison of energy-minimized structures of (***S***)-**10g** and previously reported solution conformation of **2** revealed that three functional groups on the indole template well overlapped the three pharmacophore residues of **2** as expected. In this model, indole scaffold favorably mimicked the backbone of Arg–Arg–Nal sequence of **2** (see Fig. 4).

In summary, a series of indole-based compounds were designed, synthesized, and characterized as a novel class of CXCR4 antagonists. Although their IC_{50} values are in the μM range, these indole derivatives could serve as a useful lead for further medicinal chemistry programs.

Table 2
IC_{50} values of selected indole derivatives

Compound	Structure	IC_{50} (μM)
10d	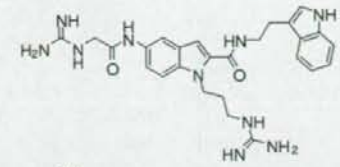	3.0
10f	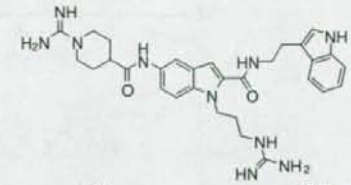	3.0
(***S***)-**10g**	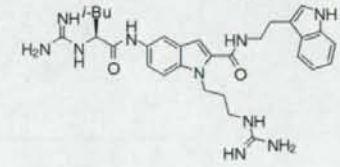	1.2
(***R***)-**10g**	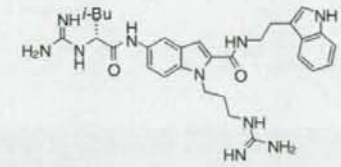	2.2
(***S***)-**10h**	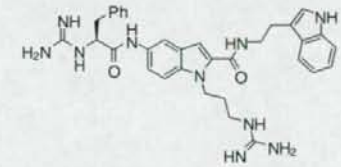	1.7
(***R***)-**10h**	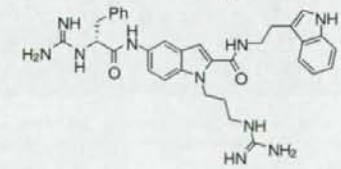	3.7
10i	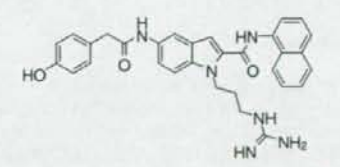	4.8
13b	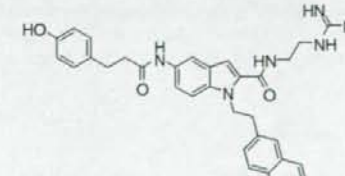	2.7
2	Cyclo(-D-Tyr–Arg–Arg–Nal–Gly–)	0.035

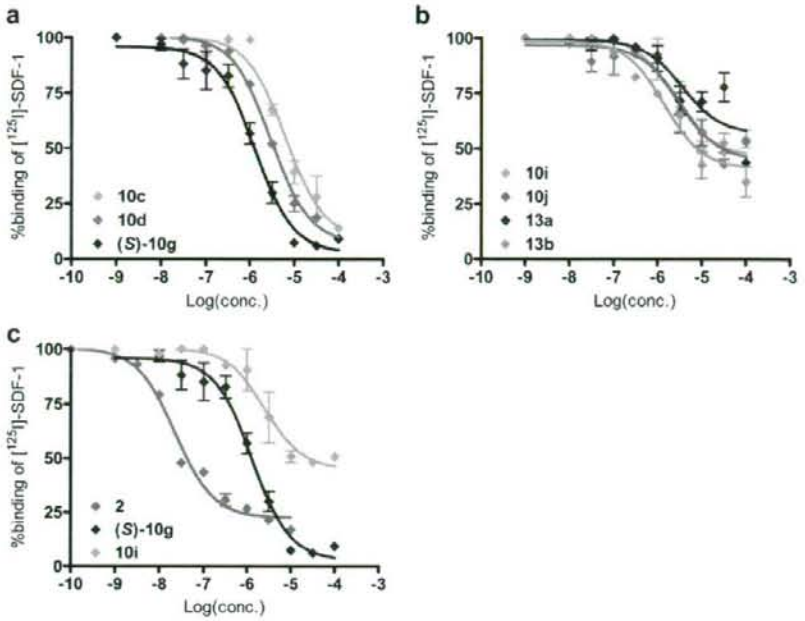

Figure 3. Ligand binding dose response of the compounds (a) having two guanidino pharmacophores and (b) having a phenol pharmacophore, and (c) the comparison of the two subsets with the parent peptide **2**.

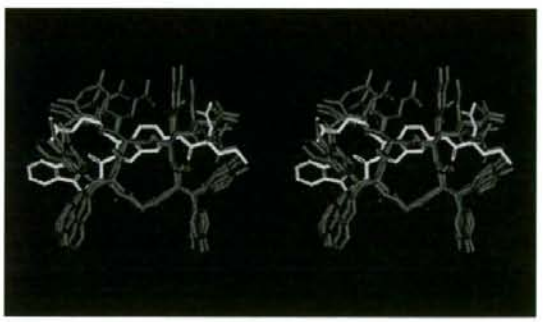

Figure 4. Overlay of a low-energy structure of (***S***)-**10g** (green) and **2** (gray). The molecular modeling of (***S***)-**10g** was performed using MacroModel-Program (Ver. 8.1) with 'MMFF' force field.

Acknowledgments

This work was supported by Grant-in-Aid for Scientific Research and Targeted Proteins Research Program from the Ministry of Education, Culture, Sports, Science, and Technology of Japan, and Health and Labour Sciences Research Grants (Research on HIV/AIDS). Computation time was provided by the Supercomputer Laboratory, Institute for Chemical Research, Kyoto University. S.U. and S.I. are grateful to the JSPS Research Fellowships for Young Scientists.

References and notes

1. Müller, A.; Homey, B.; Soto, H.; Ge, N.; Catron, D.; Buchanan, M. E.; Mcclanahan, T.; Murphy, E.; Yuan, W.; Wagner, S. M.; Barrera, J. L.; Mohar, A.; Verástegui, E.; Zlotnik, A. *Nature* **2001**, *410*, 50.
2. Nanki, T.; Hayashida, K.; El-Gabalawy, H. S.; Suson, S.; Shi, K.; Girschick, H. J.; Yavuz, S.; Lipsky, P. E. *J. Immunol.* **2000**, *165*, 6590.
3. Oberlin, E.; Amara, A.; Bachelerie, F.; Bessia, C.; Virelizier, J. L.; Arenzana-Seisdedos, F.; Schwartz, O.; Heard, J. M.; Clark-Lewis, I.; Legler, D. L.; Loetscher, M.; Baggiolini, M.; Moser, B. *Nature* **1996**, *382*, 833.
4. Masuda, M.; Nakashima, H.; Ueda, T.; Naba, H.; Ikoma, R.; Otaka, A.; Terakawa, Y.; Tamamura, H.; Ibuka, T.; Murakami, T.; Koyanagi, Y.; Waki, M.; Matsumoto, A.; Yamamoto, N.; Funakoshi, S.; Fujii, N. *Biochem. Biophys. Res. Commun.* **1992**, *189*, 845.
5. Fujii, N.; Oishi, S.; Hiramatsu, K.; Araki, T.; Ueda, S.; Tamamura, H.; Otaka, A.; Kusano, S.; Terakubo, S.; Nakashima, H.; Broach, J. A.; Trent, J. O.; Wang, Z.; Peiper, S. C. *Angew. Chem. Int. Ed.* **2003**, *42*, 3251.
6. Tamamura, H.; Xu, Y.; Hattori, T.; Zhang, X.; Arakaki, R.; Kanbara, K.; Omagari, A.; Otaka, A.; Ibuka, T.; Yamamoto, N.; Nakashima, H.; Fujii, N. *Biochem. Biophys. Res. Commun.* **1998**, *253*, 877.
7. (a) Tamamura, H.; Hori, A.; Kanzaki, N.; Hiramatsu, K.; Mizumoto, M.; Nakashima, H.; Yamamoto, N.; Otaka, A.; Fujii, N. *FEBS Lett.* **2003**, *550*, 79; (b) Takenaga, M.; Tamamura, H.; Hiramatsu, K.; Nakamura, N.; Yamaguchi, Y.; Kitagawa, A.; Kawai, S.; Nakashima, H.; Fujii, N.; Igarashi, R. *Biochem. Biophys. Res. Commun.* **2004**, *320*, 226.
8. Tamamura, H.; Fujisawa, M.; Hiramatsu, K.; Mizumoto, M.; Nakashima, H.; Yamamoto, N.; Otaka, A.; Fujii, N. *FEBS Lett.* **2004**, *569*, 99.
9. (a) Donzella, G. A.; Schols, D.; Lin, S. W.; Este, J. A.; Nagashima, K. A.; Maddon, P. J. *Nat. Med.* **1998**, *4*, 72; (b) Ichiya, K.; Yokoyama-Kumakura, S.; Tanaka, Y.; Tanaka, R.; Hirose, K.; Bannai, K.; Edamatsu, T.; Yanaka, M.; Niitani, Y.; Miyano-Kurosaki, N.; Takaku, H.; Koyanagi, Y.; Yamamoto, N. *Proc. Natl. Acad. Sci. U.S.A.* **2003**, *100*, 4185; (c) Tamamura, H.; Ojida, A.; Ogawa, T.; Tsutsumi, H.; Masuno, H.; Nakashima, H.; Yamamoto, N.; Hamachi, I.; Fujii, N. *J. Med. Chem.* **2006**, *49*, 3412; (d) Zhan, W.; Liang, Z.; Zhu, A.; Kurtkaya, S.; Shim, H.; Snyder, J. P.; Liotta, D. C. *J. Med. Chem.* **2007**, *50*, 5655.
10. Conversion of peptide to nonpeptide by scaffolding strategy, see: (a) Hirschmann, R.; Nicolaou, K. C.; Pietranico, S.; Salvino, J.; Leahy, E. M.; Sprengeler, P. A.; Furst, G.; Strader, C. D.; Cascieri, M. A.; Candelore, M. R.; Donaldson; Cindy; Vale, W.; Maechler, L. *J. Am. Chem. Soc.* **1992**, *114*, 9217; (b) Kawato, H. C.; Nakayama, K.; Inagaki, H.; Ohta, T. *Org. Lett.* **2001**, *3*, 3451; (c) Nakayama, K.; Kawato, H. C.; Inagaki, H.; Ohta, T. *Org. Lett.* **2001**, *3*, 3447.
11. (a) Ueda, S.; Oishi, S.; Wang, Z.-x.; Araki, T.; Tamamura, H.; Cluzeau, J.; Ohno, H.; Kusano, S.; Nakashima, H.; Trent, J. O.; Peiper, S. C.; Fujii, N. *J. Med. Chem.* **2007**, *50*, 192; (b) Tamamura, H.; Araki, T.; Ueda, S.; Wang, Z.; Oishi, S.; Esaka, A.; Trent, J. O.; Nakashima, H.; Yamamoto, N.; Peiper, S. C.; Otaka, A.; Fujii, N. *J. Med. Chem.* **2005**, *48*, 3280.
12. Distances (Å) between β-carbons of **2** during 1000 ps MD calculation; D-Tyr^1–Arg^3: 8.0–9.2, D-Tyr^1–Nal^4: 7.9–9.1, Arg^3–Nal^4: 4.7–5.4, Arg^2–Arg^3: 4.5–5.3, Arg^2–Nal^4: 7.3–8.4, Arg^3–Nal^4: 4.7–5.4. Distances (Å) between two key atoms of energy-minimized 5-acetamido-1-methylindole-2-carboxamide:

(acetamide N)-(*N*-methyl C), 6.7; (acetamide N)-(carboxamide N), 8.1; (methyl C)-(carboxamide N), 4.5.

13. Compound (*S*)-**10g**: $[\alpha]_D^{23}$ −6.4(c0.35, CH_3OH); ^1H NMR (500 MHz, DMSO-d_6): δ = 0.93 (d, *J* = 6.0 Hz, 3H), 0.95 (d, *J* = 5.9 Hz, 3H), 1.60–1.76 (m, 3H), 1.92 (tt, *J* = 6.6, 7.2 Hz, 2H), 2.97 (t, *J* = 7.6 Hz, 2H), 3.14 (dt, *J* = 6.2, 6.6 Hz, 2H), 3.55 (dt, *J* = 6.7, 7.0 Hz, 2H), 4.26–4.41 (m, 1H), 4.55 (t, *J* = 7.2 Hz, 2H), 6.86–7.53 (brm, 8H), 6.99 (m, 1H), 7.03–7.11 (m, 2H), 7.20 (br, 1H), 7.33–7.43 (m, 2H), 7.55 (d, *J* = 9.0 Hz, 1H), 7.59 (d, *J* = 7.9 Hz, 1H), 7.73 (t, *J* = 5.4 Hz, 1H), 7.90 (d, *J* = 9.0 Hz, 1H), 7.95–7.99, (br, 1H), 8.65 (t, *J* = 5.7 Hz, 1H), 10.08 (s, 1H), 10.82 (s, 1H); LRMS (FAB): 573 (MH^+, base peak), 444; HRMS (FAB): calcd for $C_{30}H_{41}N_{10}O_2$ (MH^+) 573.3414; found 573.3418. Compound (*S*)-**10h**: $[\alpha]_D^{23}$ 3.3(c0.34, CH_3OH); ^1H NMR (500 MHz, DMSO-d_6): δ = 1.91 (tt, *J* = 7.2, 7.4 Hz, 2H), 2.96 (t, *J* = 7.3 Hz, 2H), 2.97–3.04 (m, 1H), 3.13 (dt, *J* = 5.4, 7.2 Hz, 2H), 3.20–3.27 (m, 1H), 3.54 (dt, *J* = 6.0, 7.3 Hz, 2H), 4.54 (t, *J* = 7.4 Hz, 2H), 4.56–4.62 (m, 1H), 6.78–7.64 (brm, 8H), 6.98 (m, 1H), 7.03–7.10 (m, 2H), 7.19 (m, 1H), 7.21–7.27 (m, 1H), 7.27-7.40 (m, 6H), 7.55 (d, *J* = 8.9 Hz, 1H), 7.58 (d, *J* = 7.7 Hz, 1H), 7.71 (t, *J* = 5.3 Hz, 1H), 7.85 (d, *J* = 8.9 Hz, 1H), 7.89–7.92, (br, 1H), 8.64 (t, *J* = 6.0 Hz, 1H), 10.12 (br, 1H), 10.82 (br, 1H); LRMS (FAB): 607 (MH^+, base peak), 444; HRMS (FAB): calcd for $C_{33}H_{39}N_{10}O_2$ (MH^+) 607.3257; found 607.3251.
14. Tamamura, H.; Hiramatsu, K.; Ueda, S.; Wang, Z.; Kusano, S.; Terakubo, S.; Trent, J. O.; Peiper, S. C.; Yamamoto, N.; Nakashima, H.; Otaka, A.; Fujii, N. *J. Med. Chem.* **2005**, *48*, 380.

Bioorganic & Medicinal Chemistry 16 (2008) 9184–9187

Contents lists available at ScienceDirect

Bioorganic & Medicinal Chemistry

journal homepage: www.elsevier.com/locate/bmc

Identification of minimal sequence for HIV-1 fusion inhibitors

Hiroki Nishikawa [a], Shinya Oishi [a], Mizuno Fujita [a], Kentaro Watanabe [a], Rei Tokiwa [a], Hiroaki Ohno [a], Eiichi Kodama [b], Kazuki Izumi [b], Keiko Kajiwara [b], Takeshi Naitoh [b], Masao Matsuoka [b], Akira Otaka [a,c], Nobutaka Fujii [a,*]

[a] Graduate School of Pharmaceutical Sciences, Kyoto University, Sakyo-ku, Kyoto 606-8501, Japan
[b] Laboratory of Virus Control, Institute for Virus Research, Kyoto University, Sakyo-ku, Kyoto 606-8507, Japan
[c] Graduate School of Pharmaceutical Sciences, The University of Tokushima, Tokushima 770-8505, Japan

ARTICLE INFO

Article history:
Received 7 August 2008
Revised 29 August 2008
Accepted 5 September 2008
Available online 10 September 2008

Keywords:
HIV-1
Fusion inhibitor
α-Helix
Heptad repeat

ABSTRACT

Emergence of multi-drug resistant HIV-1 is a serious problem for AIDS treatment. Recently, the virus-cell membrane fusion process has been identified as a promising target for the development of novel drugs against these resistant variants. In this study, we identified a 29-residue peptide fusion inhibitor, SC29EK, which shows activity comparable to the previously reported inhibitor SC35EK. Some residues in SC29EK not required for interaction with virus gp41 heptad repeat 1 (HR1) were replaced with a non-proteinogenic amino acid, 2-aminoisobutyric acid (Aib), to stabilize the α-helix structure and to provide resistance to peptidases.

1. Introduction

Emergence of HIV-1 variants resistant to clinically approved inhibitors such as reverse transcriptase (RT) or viral protease is a serious problem in AIDS treatment.[1] Therefore, development of novel anti-HIV-1 drugs suppressing such resistant variants is urgently required. In this regard, inhibitors that target other processes, including integration, receptor binding or fusion have been proposed to suppress such resistant variants.[2–6] We and others have recently focused on viral fusion to host cells for development of novel anti-HIV agents that effectively inhibit HIV-1 replication with fewer resistant variants and adverse side effects.[7–9] Among envelope glycoproteins, gp41 in particular plays a pivotal role in the fusion process. Briefly, gp41 in trimer anchors to the host cell membrane, and two extra-virion α-helical regions, designated as heptad repeats 1 and 2 (HR1 and HR2), form an anti-parallel 6-helix bundle by the interaction between HR1 and HR2, leading to fusion of HIV-1 with the cell membrane.[10]

Enfuvirtide (T-20) **1**, which is derived from the gp41 HR2 region, is the only clinically approved peptide fusion inhibitor.[11] Although this agent is effective against variants resistant to multiple RT- and protease-inhibitors as well as wild-type strains,[12,13] T-20-resistant HIV-1 strains have emerged after T-20-containing therapy.[14,15] Thus, the development of second generation fusion inhibitors that suppress T-20-resistant variants is urgently needed. T-20 **1** and another HR2 peptide C34 **2** show the anti-HIV activity by binding with the viral gp41 HR1 to disturb the 6-helix bundle formation (Table 1).[10a] Previously, we developed the novel potent fusion inhibitors T-20EK[16] **3** and SC35EK[9] **4**, which are derived from T-20 **1** and C34 **2**, respectively. On the basis of the α-helical structure of these HR2 peptides upon binding with HR1,[17] we distinguished two surfaces: a virus HR1 interactive site and a solvent-accessible site (Fig. 1). For the residues at the solvent-accessible site (b, c, f, and g in Fig. 1), a series of systematic replacements with hydrophilic glutamic acid (E) or lysine (K) was introduced (EK motif) to enhance the α-helicity of the HR2 peptides by possible intrahelical salt-bridges. On the other hand, the residues at the interactive site (a, d, and e in Fig. 1) were retained for binding affinity. The stabilized bioactive α-helix conformation led to increased anti-HIV-1 activity through higher affinity with the virus HR1 region. 2-Aminoisobutyric acid (Aib), which could enhance and/or stabilize α-helicity of the peptides,[18,19] and may confer peptidase resistance,[20] was also applied to the modification of α-helix inducible EK motifs.

In this study, we investigated the minimal sequence of C34 **2** and SC35EK **4** for potent anti-HIV activity. In addition, modifications of each EK motif with Aib-containing motifs were examined.

2. Results and discussion

We and other groups have reported that C34 **2** and its derivatives interact with N36, a representative peptide of the gp41 HR1

* Corresponding author. Tel.: +81 75 753 4551; fax: +81 75 753 4570.
E-mail address: nfujii@pharm.kyoto-u.ac.jp (N. Fujii).

0968-0896/$ - see front matter © 2008 Elsevier Ltd. All rights reserved.
doi:10.1016/j.bmc.2008.09.018

Table 1
Sequences and anti-HIV activities of C34 and its derivatives, and T_m values of the mixture with N36

Peptide		Sequence	EC_{50} (nM)[a]	T_m (°C)[b]
T-20	**1**	YTSLIHSLIEESQNQQEKNEQELLELDKWASLWNWF	15	ND[c]
C34	**2**	WMEWDREINNYTSLIHSLIEESQNQQEKNEQELL	0.68	52.5
T-20EK	**3**	YTSLI**EE**LI**KK**S**EE**QQ**KK**N**EE**L**KK**L**EE**WA**KK**WNWF	1.8	N.D.[c]
SC35EK	**4**	W**EE**WD**KK**I**EE**YT**KK**I**EE**LI**KK**S**EE**QQ**KK**N**EE**L**KK**	0.39	71.5
C29	**5**	WMEWDREINNYTSLIHSLIEESQNQQEKN	46	48.5
C22	**6**	WMEWDREINNYTSLIHSLIEES	>1000	38.5
SC29EK	**7**	W**EE**WD**KK**I**EE**YT**KK**I**EE**LI**KK**S**EE**QQ**KK**N	0.46	65.0
SC22EK	**8**	W**EE**WD**KK**I**EE**YT**KK**I**EE**LI**KK**S	60	63.5

[a] EC_{50} was determined as the concentration that blocked HIV-1 replication by 50%.
[b] T_m values were defined by the midpoint of the thermal unfolding transition state (Fig. 4).
[c] ND, not determined.

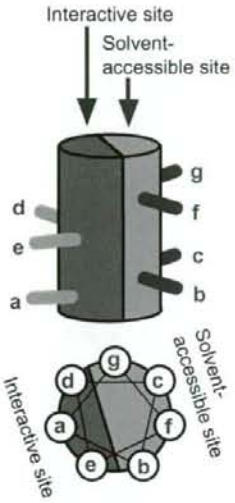

Figure 1. The design concept and helical wheel representation of HIV-1 gp41 HR2 peptide analogues. In the heptad repeat of α-helix, positions a, d, e and positions b, c, f, g represent the viral HR1 interactive and solvent-accessible site, respectively.

region.[9,19,21] In these reports, N-terminal tryptophan rich domain (WRD) containing two tryptophan residues of C34 **2** is essential for the interaction with the HR1 region,[22] while the C-terminal sequence might not be important compared to the N-terminal.[19,23] In order to identify the minimal N-terminal sequence of C34 **2** and SC35EK **4**, we designed two C-terminally truncated peptides C29 **5** and C22 **6** as well as the EK-motif-containing congeners SC29EK **7** and SC22EK **8**, respectively (Table 1). The anti-HIV activity of these peptides was examined by MAGI assay.[24,25] C29 **5** and C22 **6** showed marginal activity compared to the original C34 **2**,[19,26,27] while anti-HIV activity of SC29EK **7** possessing four EK motifs was comparable to that of C34 **2** and SC35EK **4**. Further truncation of an EK motif resulted in a significant decrease in anti-HIV activity (SC22EK **8**; EC_{50} = 60 nM). It is of note that SC29EK **7** and SC22EK **8** with EK motifs showed more potent activity than the original peptides C29 **5** and C22 **6**, respectively.

The potent anti-HIV activity of HR2-derived fusion inhibitors can be rationalized by the facilitated bioactive α-helix conformation, which is favorable for binding with the gp41 HR1 region.[9,28] Wavelength-dependent circular dichroism (CD) spectra of SC29EK **7** at 25 °C showed characteristic spectrum minima at 208 and 222 nm, which indicate the presence of a stable α-helical conformation, as observed in SC35EK **4** (Fig. 2). On the other hand, SC22EK **8** showed slightly less α-helicity compared with SC35EK **4** and SC29EK **7**, indicating that the truncated sequence of **8** may be insufficient to stabilize the α-helix structure. Native peptides, C34 **2**, C29 **5**, and C22 **6** exhibited similar spectra indicating the random structure (Fig. 2).

The binding affinities were estimated by measuring the CD spectra of HR2 peptides **2** and **4–8** in the presence of equimolar amount of N36 (HR1 region peptide). Similar spectra were observed in all N36/C34 derivative complexes except for the N36/C22 **6** complex, indicating that these peptide mixtures contained the similar stable 6-helix conformation at 25 °C (Fig. 3). Less stable coiled-coil structure of the N36/C22 **6** complex was consistent with the deficient anti-HIV activity of C22 **6**. Thermal stabilities of possible 6-helix bundle structures consisting of N36 and C34 derivatives were also evaluated by monitoring the CD signal at 222 nm. Melting temperature (T_m) of the complex was defined as the midpoint of thermal unfolding transition state shown in CD profiles (Fig. 4). T_m values of N36/SC35EK **4**, N36/SC29EK **7**, and N36/SC22EK **8** mixtures were 71.5, 65.0, and 63.5 °C, respectively, which were higher than those of the corresponding mixtures of native sequences [T_m (N36/C34 **2**) = 52.5 °C, T_m (N36/C29 **5**) = 48.5 °C, and T_m (N36/C22 **6**) = 38.5 °C] (Fig. 4). These results indicate that the introduction of EK motifs to HR2 peptides enhances binding affinity with the HR1 region, which could provide more potent anti-HIV activity. It should be noted that SC22EK **8** showed less potent anti-HIV activity compared with the other EK motif-containing peptides, although the thermal stabilities were similar. The limited coverage of the HR1 region by the truncated sequence of **8** may be inadequate for complete inhibition against folding of viral gp41 even with high binding affinity. As such, the potent anti-HIV activity of SC29EK **7** is rationalized by the presence of minimal interactive residues as well as the stabilized bioactive α-helix conformation induced by EK motifs.

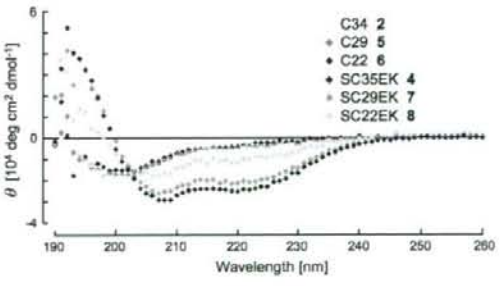

Figure 2. CD spectra of HR2 peptide analogues.

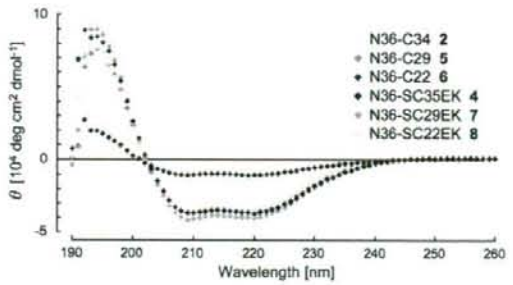

Figure 3. CD spectra of HR2 peptide analogues in the presence of equimolar amount of N36.

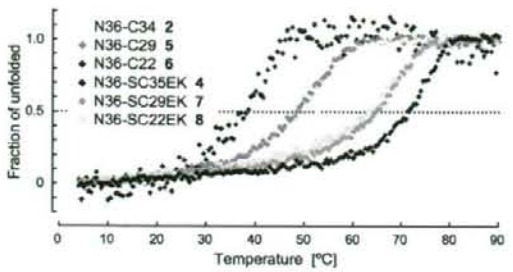

Figure 4. Thermal midpoint analysis of CD signal at 222 nm for HR1 (N36) and HR2 peptide complex.

Since the residues at the solvent-accessible sites of HR2 peptides have no direct involvement in the interaction with the viral HR1 region, we expected that these EK motifs could be replaced with other α-helix-inducible units. Replacement of a part of the EK motifs in SC29EK **7** with a pair of Aib-containing dipeptides such as Aib-Glu (***aE***) and Aib-Lys (***aK***) was attempted (peptides **9–12**, Fig. 5 and Table 2).[18,20] Anti-HIV activities of the Aib-substituted peptides **9–12** were equipotent or lower compared with SC29EK **7**. Peptide **9**, which was modified with a pair of ***aE*** and ***aK*** dipeptides at the essential WRD of the HR2 peptide[22] was the most potent, with the bioactivity almost identical to that of the parent SC29EK **7** (Table 2). This indicated that EK residues could be replaced with non-proteinogenic and α-helix inducible Aib residues, which may also enhance the biostability in vivo. In order to investigate the effect of the remaining Glu-Lys pairing in the ***aE/aK*** motif, we further substituted these residues with glycine (Gly)

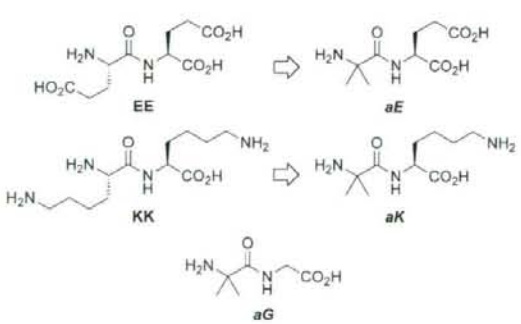

Figure 5. Substitution of an EE or KK unit with Aib-Glu (***aE***), Aib-Lys (***aK***), or Aib-Gly (***aG***).

Table 2
Sequences and anti-HIV activities of SC29EK analogues containing aminoisobutyric acid (Aib) residue

Peptide	Sequence	EC_{50}[a] (nM)
7	WEEWDKKIEEYTKKIEELIKKSEEQQKKN	0.46
9	Wa*E*WD*aK*IEEYTKKIEELIKKSEEQQKKN	0.54
10	WEEWDKKI*aE*YT*aK*IEELIKKSEEQQKKN	2.15
11	WEEWDKKIEEYTKKI*aE*LI*aK*SEEQQKKN	0.87
12	WEEWDKKIEEYTKKIEELIKKS*aE*QQ*aK*N	7.10
13	Wa*G*WD*aG*IEEYTKKIEELIKKSEEQQKKN	37.5
14	WEEWDKKI*aG*YT*aG*IEELIKKSEEQQKKN	270
15	WEEWDKKIEEYTKKI*aG*LI*aG*SEEQQKKN	25.6
16	WEEWDKKIEEYTKKIEELIKKS*aG*QQ*aG*N	31.3

[a] EC_{50} was determined as the concentration that blocked HIV-1 replication by 50%.

(peptides **13–16**) (Fig. 5 and Table 2). All substituted peptides **13–16** showed significantly less potent anti-HIV activity compared with the corresponding peptides **9–12** containing an ***aE/aK*** motif (Table 2), suggesting that modification of an EK motif with two Aib-Gly (***aG***) is not suitable for potent anti-HIV activity.

3. Conclusions

In this study, we identified the minimal bioactive sequence of HIV-1 fusion inhibitors and developed a novel potent fusion inhibitory peptide SC29EK **7** based on the previously reported SC35EK **4**. SC29EK **7** reproduced potent anti-HIV-1 activity comparable to SC35EK **4**. The introduction of α-helix-inducible EK motifs to less potent C29 **5** recovered the bioactivity of the parent C34 **2**, indicating that binding of the C29 sequence containing essential tryptophan rich domain to the gp41 HR1 is sufficient for anti-HIV activity. Moreover, it was also demonstrated that some EK motifs are replaceable with other non-proteinogenic amino acids such as 2-aminoisobutyric acid (Aib). These results may lead to development of more potent HIV-1 fusion inhibitors.

4. Experimental

4.1. Peptide synthesis

Protected peptide-resins were manually constructed by Fmoc-based solid-phase peptide synthesis. *t*-Bu ester for Asp and Glu; 2,2,4,6,7-pentamethyldihydrobenzofuran-5-sulfonyl (Pbf) for Arg; *t*-Bu for Thr; Tyr and Ser; Boc for Lys; and Trt for Gln, Asn, and His were employed for side-chain protection. Fmoc-amino acids were coupled using five equivalents of reagents [Fmoc-amino acid, *N,N'*-diisopropylcarbodiimide (DIPCDI), and HOBt·H_2O] in DMF for 1.5 h. Fmoc deprotection was performed with 20% piperidine in DMF (2 × 1 min, 1 × 20 min). The resulting protected resin was treated with TFA/thioanisole/*m*-cresol/1,2-ethandithiol/H_2O (80:5:5:5:5) at room temperature for 2 h. After removal of the resin by filtration, the filtrate was poured into ice-cold dry diethyl ether. The resulting powder was collected by centrifugation and washed with ice-cold dry diethyl ether. The crude product was purified by preparative HPLC on a Cosmosil 5C18-ARII preparative column (Nacalai Tesque, 20 × 250 mm, flow rate 10 mL/min) to afford the expected peptides. All peptides were characterized by an ESI-MS (Sciex API*III*E, Toronto, Canada) or MALDI-TOF-MS (AXIMA-CFR plus, Shimadzu, Kyoto, Japan), and the purity was calculated as >95% by HPLC on a Cosmosil 5C18-ARII analytical column (Nacalai Tesque, 4.6 × 250 mm, flow rate 1 mL/min) at 220 nm absorbance. The detailed MS data are shown in Table 3.

Table 3
Mass spectrum data of synthesized peptides

Peptide	Calculated MW (M+H$^+$)		Observed MW
1	$C_{204}H_{302}N_{51}O_{64}$	4492.9	4492.5[a]
2	$C_{186}H_{284}N_{51}O_{64}S$	4290.6	4289.3[a]
3	$C_{213}H_{329}N_{52}O_{63}$	4626.2	4625.5[a]
4	$C_{203}H_{326}N_{51}O_{66}$	4537.1	4536.3[a]
5	$C_{159}H_{240}N_{45}O_{54}S$	3677.9	3677.7[a]
6	$C_{125}H_{185}N_{32}O_{40}S$	2808.1	2808.1[a]
7	$C_{170}H_{270}N_{43}O_{54}$	3780.2	3779.5[a]
8	$C_{134}H_{210}N_{31}O_{40}$	2895.3	2895.2[a]
9	$C_{167}H_{265}N_{42}O_{52}$	3693.1	3693.5[b]
10	$C_{167}H_{265}N_{42}O_{52}$	3693.1	3693.5[b]
11	$C_{167}H_{265}N_{42}O_{52}$	3693.1	3692.5[b]
12	$C_{167}H_{265}N_{42}O_{52}$	3693.1	3693.8[b]
13	$C_{160}H_{252}N_{41}O_{50}$	3550.0	3550.1[b]
14	$C_{160}H_{252}N_{41}O_{50}$	3550.0	3549.5[b]
15	$C_{160}H_{252}N_{41}O_{50}$	3550.0	3550.2[b]
16	$C_{160}H_{252}N_{41}O_{50}$	3550.0	3550.2[b]

[a] MALDI-TOF-MS.
[b] ESI-MS (reconstructed).

4.2. Viruses and cells

An infectious clone pNL4-3 (GenBank Accession No. AF324493) was used for the construction and production of HIV-1 as described previously.[29] A wild-type HIV-1 was generated by transfection of pNL4-3 into 293T cells. HeLa-CD4-LTR-β-gal cells (MAGI cells) were kindly provided by Dr. Emerman through the AIDS Research and Reference Reagent Program, Division of AIDS, National Institute of Allergy and Infectious Disease (NIAID) (Bethesda, MD, USA).

4.3. Anti-HIV-1 activity

Anti-HIV-1 activity was determined by the multinuclear activation of a galactosidase indicator (MAGI) assay as described previously.[24,25] Briefly, the MAGI cells (10^4 cells/well) were seeded in flat bottomed 96-well microtitre plates. The following day, the cells were inoculated with HIV-1 (60 MAGI units/well, yielding 60 blue cells after 48 h incubation) and cultured in the presence of various concentrations of peptide inhibitors in fresh medium. After 48 h incubation, all the blue cells stained with 5-bromo-4-chloro-3-indolyl-β-D-galactopyranoside (X-gal) in each well were counted. The activity of inhibitors was determined as the concentration that blocked HIV-1 replication by 50% (50% effective concentration [EC_{50}]).

4.4. CD measurement

An HR2 peptide (peptides **2** and **4**–**8**) was dissolved in PBS pH 7.4 at a concentration of 10 μM. At the CD measurement of mixture of an HR1 peptide (N36) and an HR2 peptide or its analogues, the peptides were incubated at 37 °C for 30 min (final concentration of both HR1 peptide and HR2 peptide was 10 μM in PBS, pH 7.4). The wavelength-dependent of molar ellipticity [θ] was monitored at 25 °C as the average of eight scans, and the thermal stability of the HR1 and HR2 mixture was estimated by monitoring the change in the CD signal at 222 nm in a spectropolarimeter (Model J-710; Jasco, Tokyo, Japan) equipped with a thermoelectric temperature controller. The midpoint of thermal unfolding transition (melting temperature [T_m]) of each complex was determined as described previously.[9]

Acknowledgments

This work was supported in part by grants for the Promotion of AIDS Research from the Ministry of Health and Welfare and the Ministry of Education, Culture, Sports, Science, and Technology of Japan (E.K. and S.O.); a grant for Research for Health Sciences Focusing on Drug Innovation from The Japan Health Sciences Foundation (E.K., S.O., N.F., and M.M.); and the 21st Century COE program "Knowledge Information Infrastructure for Genome Science" (N.F. and H.N.). H.N. is grateful for the JSPS Research Fellowships for Young Scientists. Appreciation is expressed to Mr. Maxwell Reback (Kyoto University) for reading the manuscript.

References and notes

1. Clavel, F.; Hance, A. J. *N. Engl. J. Med.* **2004**, *350*, 1023.
2. Fatkenheuer, G.; Pozniak, A. L.; Johnson, M. A.; Plettenberg, A.; Staszewski, S.; Hoepelman, A. I.; Saag, M. S.; Goebel, F. D.; Rockstroh, J. K.; Dezube, B. J.; Jenkins, T. M.; Medhurst, C.; Sullivan, J. F.; Ridgway, C.; Abel, S.; James, I. T.; Youle, M.; van der Ryst, E. *Nat. Med.* **2005**, *11*, 1170.
3. Grinsztejn, B.; Nguyen, B. Y.; Katlama, C.; Gatell, J. M.; Lazzarin, A.; Vittecoq, D.; Gonzalez, C. J.; Chen, J.; Harvey, C. M.; Isaacs, R. D. *Lancet* **2007**, *369*, 1261.
4. Hazuda, D. J.; Young, S. D.; Guare, J. P.; Anthony, N. J.; Gomez, R. P.; Wai, J. S.; Vacca, J. P.; Handt, L.; Motzel, S. L.; Klein, H. J.; Dornadula, G.; Danovich, R. M.; Witmer, M. V.; Wilson, K. A.; Tussey, L.; Schleif, W. A.; Gabryelski, L. S.; Jin, L.; Miller, M. D.; Casimiro, D. R.; Emini, E. A.; Shiver, J. W. *Science* **2004**, *305*, 528.
5. Root, M. J.; Kay, M. S.; Kim, P. S. *Science* **2001**, *291*, 884.
6. Tagat, J. R.; McCombie, S. W.; Nazareno, D.; Labroli, M. A.; Xiao, Y.; Steensma, R. W.; Strizki, J. M.; Baroudy, B. M.; Cox, K.; Lachowicz, J.; Varty, G.; Watkins, R. *J. Med. Chem.* **2004**, *47*, 2405.
7. Bewley, C. A.; Louis, J. M.; Ghirlando, R.; Clore, G. M. *J. Biol. Chem.* **2002**, *277*, 14238.
8. Dwyer, J. J.; Wilson, K. L.; Davison, D. K.; Freel, S. A.; Seedorff, J. E.; Wring, S. A.; Tvermoes, N. A.; Matthews, T. J.; Greenberg, M. L.; Delmedico, M. K. *Proc. Natl. Acad. Sci. U.S.A.* **2007**, *104*, 12772.
9. Otaka, A.; Nakamura, M.; Nameki, D.; Kodama, E.; Uchiyama, S.; Nakamura, S.; Nakano, H.; Tamamura, H.; Kobayashi, Y.; Matsuoka, M.; Fujii, N. *Angew. Chem. Int. Ed. Engl.* **2002**, *41*, 2937.
10. (a) Chan, D. C.; Kim, P. S. *Cell* **1998**, 93, 681; (b) Eckert, D. M.; Kim, P. S. *Annu. Rev. Biochem.* **2001**, *70*, 777.
11. Matthews, T.; Salgo, M.; Greenberg, M.; Chung, J.; DeMasi, R.; Bolognesi, D. *Nat. Rev. Drug Discov.* **2004**, 3, 215.
12. Lalezari, J. P.; Henry, K.; O'Hearn, M.; Montaner, J. S.; Piliero, P. J.; Trottier, B.; Walmsley, S.; Cohen, C.; Kuritzkes, D. R.; Eron, J. J., Jr.; Chung, J.; DeMasi, R.; Donatacci, L.; Drobnes, C.; Delehanty, J.; Salgo, M. *N. Engl. J. Med.* **2003**, *348*, 2175.
13. Lazzarin, A.; Clotet, B.; Cooper, D.; Reynes, J.; Arasteh, K.; Nelson, M.; Katlama, C.; Stellbrink, H. J.; Delfraissy, J. F.; Lange, J.; Huson, L.; DeMasi, R.; Wat, C.; Delehanty, J.; Drobnes, C.; Salgo, M. *N. Engl. J. Med.* **2003**, *348*, 2186.
14. Poveda, E.; Rodes, B.; Toro, C.; Martin-Carbonero, L.; Gonzalez-Lahoz, J.; Soriano, V. *AIDS* **2002**, *16*, 1959.
15. Wei, X.; Decker, J. M.; Liu, H.; Zhang, Z.; Arani, R. B.; Kilby, J. M.; Saag, M. S.; Wu, X.; Shaw, G. M.; Kappes, J. C. *Antimicrob. Agents Chemother.* **2002**, *46*, 1896.
16. Oishi, S.; Ito, S.; Nishikawa, H.; Watanabe, K.; Tanaka, M.; Ohno, H.; Izumi, K.; Sakagami, Y.; Kodama, E.; Matsuoka, M.; Fujii, N. *J. Med. Chem.* **2008**, *51*, 388.
17. Chan, D. C.; Fass, D.; Berger, J. M.; Kim, P. S. *Cell* **1997**, *89*, 263.
18. Karle, I. L.; Balaram, P. *Biochemistry* **1990**, *29*, 6747.
19. Sia, S. K.; Carr, P. A.; Cochran, A. G.; Malashkevich, V. N.; Kim, P. S. *Proc. Natl. Acad. Sci. U.S.A.* **2002**, *99*, 14664.
20. Yamaguchi, H.; Kodama, H.; Osada, S.; Kato, F.; Jelokhani-Niaraki, M.; Kondo, M. *Biosci. Biotechnol. Biochem.* **2003**, *67*, 2269.
21. Liu, S.; Lu, H.; Niu, J.; Xu, Y.; Wu, S.; Jiang, S. *J. Biol. Chem.* **2005**, *280*, 11259.
22. Chan, D. C.; Chutkowski, C. T.; Kim, P. S. *Proc. Natl. Acad. Sci. U.S.A.* **1998**, *95*, 15613.
23. Gochin, M.; Savage, R.; Hinckley, S.; Cai, L. *Biol. Chem.* **2006**, *387*, 477.
24. Kimpton, J.; Emerman, M. *J. Virol.* **1992**, *66*, 2232.
25. Kodama, E. I.; Kohgo, S.; Kitano, K.; Machida, H.; Gatanaga, H.; Shigeta, S.; Matsuoka, M.; Ohrui, H.; Mitsuya, H. *Antimicrob. Agents Chemother.* **2001**, *45*, 1539.
26. Ji, H.; Shu, W.; Burling, F. T.; Jiang, S.; Lu, M. *J. Virol.* **1999**, *73*, 8578.
27. Shu, W.; Liu, J.; Ji, H.; Radigen, L.; Jiang, S.; Lu, M. *Biochemistry* **2000**, *39*, 1634.
28. Judice, J. K.; Tom, J. Y.; Huang, W.; Wrin, T.; Vennari, J.; Petropoulos, C. J.; McDowell, R. S. *Proc. Natl. Acad. Sci. U.S.A.* **1997**, *94*, 13426.
29. Nameki, D.; Kodama, E.; Ikeuchi, M.; Mabuchi, N.; Otaka, A.; Tamamura, H.; Ohno, M.; Fujii, N.; Matsuoka, M. *J. Virol.* **2005**, *79*, 764.

The International Journal of Biochemistry & Cell Biology 41 (2009) 891–899

Contents lists available at ScienceDirect

The International Journal of Biochemistry & Cell Biology

journal homepage: www.elsevier.com/locate/biocel

Electrostatically constrained α-helical peptide inhibits replication of HIV-1 resistant to enfuvirtide

Hiroki Nishikawa[a], Shota Nakamura[b], Eiichi Kodama[c,*], Saori Ito[a], Keiko Kajiwara[c,d], Kazuki Izumi[c], Yasuko Sakagami[c], Shinya Oishi[a], Tadayasu Ohkubo[e], Yuji Kobayashi[f], Akira Otaka[g], Nobutaka Fujii[a], Masao Matsuoka[c]

[a] Graduate School of Pharmaceutical Sciences, Kyoto University, Sakyo-ku, Kyoto 606-8501, Japan
[b] Research Institute for Microbial Diseases, Osaka University, Suita, Osaka 565-0871, Japan
[c] Laboratory of Virus Control, Institute for Virus Research, Kyoto University, Sakyo-ku, Kyoto 606-8507, Japan
[d] Institute for Virus Research, and Graduate School of Biostudies, Kyoto University, Sakyo-ku, Kyoto 606-8507, Japan
[e] Graduate School of Pharmaceutical Sciences, Osaka University, Suita, Osaka 565-0871, Japan
[f] Osaka University of Pharmaceutical Sciences, Takatsuki, Osaka 569-1094, Japan
[g] Graduate School of Pharmaceutical Sciences, The University of Tokushima, Tokushima 770-8505, Japan

ARTICLE INFO

Article history:
Received 7 July 2008
Received in revised form 19 August 2008
Accepted 22 August 2008
Available online 10 September 2008

Keywords:
HIV
Fusion
Peptide
Inhibitor
α-Helix

ABSTRACT

α-Helical peptides, such as T-20 (enfuvirtide) and C34, derived from the gp41 carboxyl-terminal heptad repeat (C-HR) of HIV-1, inhibit membrane fusion of HIV-1 and the target cells. Although T-20 effectively suppresses the replication of multi-drug resistant HIV variants both in vitro and in vivo, prolonged therapy with T-20 induces emergence of T-20 resistant variants. In order to suppress the emergence of such resistant variants, we introduced charged and hydrophilic amino acids, glutamic acid (E) and lysine (K), at the solvent accessible site of C34. In particular, the modified peptide, SC34EK, demonstrates remarkably potent inhibition of membrane fusion by the resistant HIV-1 variants as well as wild-type viruses. The activity was specific to HIV-1 and little influenced by serum components. We found a strong correlation between the anti-HIV-1 activities of these peptides and the thermostabilities of the 6-helix bundles that are formed with these peptides. We also obtained the crystal structure of SC34EK in complex with a 36 amino acid sequence (N36) comprising the amino-terminal heptad repeat of HIV-1. The EK substitutions in the sequence of SC34EK were directed toward the solvent and generated an electrostatic potential, which may result in enhanced α-helicity of the peptide inhibitor. The 6-helix bundle complex of SC34EK with N36 appears to be structurally similar to that of C34 and N36. Our approach to enhancing α-helicity of the peptide inhibitor may enable future design of highly effective and specific HIV-1 inhibitors.

1. Introduction

Enfuvirtide (T-20), which has been clinically approved as the first fusion inhibitor of HIV-1, is derived from a 36 amino acid region of the carboxyl-terminal heptad repeat (C-HR) of gp41, an HIV-1 transmembrane envelope glycoprotein, which plays central role in the fusion of HIV-1 with host cells. T-20 prevents the formation of a 6-helix bundle, which is comprised of a trimer of dimers formed from the amino-terminal heptad repeat (N-HR) and the carboxyl-terminal heptad repeat (C-HR) in an antiparallel orientation. Six-helix formation by physiological gp41 enables host cell and virus membranes to contact and fuse, enabling the virus entry into the cells. Therefore, inhibition of the formation of this 6-helix bundle prevents fusion of HIV-1 and targeted host cell membranes (Derdeyn et al., 2000; Wild et al., 1992). Notably, T-20 effectively suppresses the replication of HIV-1 variants, which are resistant to multiple reverse transcriptase and protease inhibitors, and has been used in the optimized regimens for HIV-1-infected patients harboring multi-drug resistant HIV-1 variants (Lalezari et al., 2003; Lazzarin et al., 2003).

Emergence of T-20-resistant HIV-1 was reported not only in patients receiving T-20 monotherapy in a phase I clinical trial (Wei et al., 2002), but also in patients treated with a combination of T-20

* Corresponding author at: 53 Kawaramachi Shogoin, Sakyo-ku, Kyoto 606-8507, Japan. Tel.: +81 75 751 3986; fax: +81 75 751 3986.
E-mail address: ekodama@virus.kyoto-u.ac.jp (E. Kodama).

1357-2725/$ – see front matter © 2008 Elsevier Ltd. All rights reserved.
doi:10.1016/j.biocel.2008.08.039

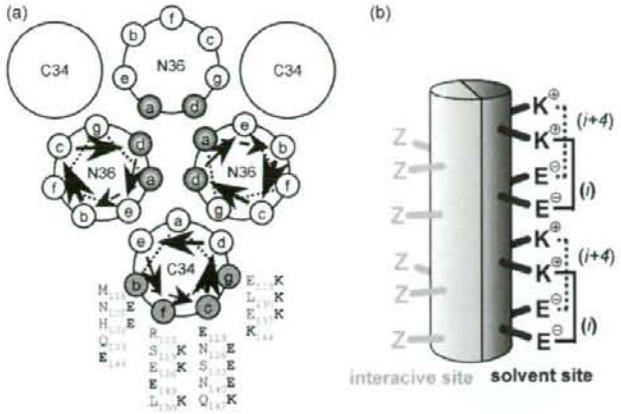

Fig. 1. Helical wheel representation of the 6-helix bundle structure and the design of SC34EK. (a) Amino acid residues at positions a, d, e of C34 are interactive sites that form the 6-helix complex with N36, while the remaining amino acid residues at positions b, c, f, g are solvent accessible sites, which are substituted with Glu (E) or Lys (K) in SC34EK. (b) The design concept of introducing the EK motif to the solvent accessible site. The α-helical C-HR peptide could be divided into interactive (red) and solvent (blue) sites. Z indicates the original amino acids of C34. Only amino acid residues at solvent sites were replaced by E at the *i* position and K at the *i*+4 position.

and other inhibitors in subsequent phases II and III trials (Matthews et al., 2004; Poveda et al., 2002). These resistant variants frequently acquired mutations in gp41, especially in amino acids 36–45 of the N-HR region (Aquaro et al., 2006; Cabrera et al., 2006; Mink et al., 2005; Poveda et al., 2002; Rimsky et al., 1998; Wei et al., 2002) (Fig. 1). Additionally, complementary mutations in the C-HR region, such as S138A mutation, were found in some T-20 resistant variants (Cabrera et al., 2006; Poveda et al., 2004; Xu et al., 2005). Introduction of these complementary mutations compensates for impaired HIV-1 replication stemming from the primary mutations that give rise to resistance. The N43D mutation in the N-HR region that confers resistance to T-20 is a well documented example (Xu et al., 2005).

Although T-20 inhibits gp41-mediated fusion (Derdeyn et al., 2000; Wild et al., 1992), it has additional effects on HIV-1 replication. For instance, baseline sensitivity of HIV-1 to T-20 is influenced not only by the amino acid sequence of gp41, but also by the co-receptor specificity (CCR5/CXCR4) defined by the structure of the V3 loop of gp120, a glycoprotein capping gp41, which binds to the CD4 cells (Derdeyn et al., 2000; Derdeyn et al., 2001). Moreover, substitutions within the CD4 binding domain of gp120 also contribute to the resistance of the virus to T-20 (Baldwin and Berkhout, 2006). Thus, the mode of action and the mechanism of resistance to T-20 seem to be complicated. In contrast, another fusion inhibitor known as C34, has been clearly shown to bind to the N-HR in vitro and act as a decoy of gp41 C-HR and prevent the formation of the 6-helix bundle (Chan et al., 1997; Liu et al., 2005; Xu et al., 2007). Its inhibitory effect is over 10-fold greater than that of T-20 (Armand-Ugon et al., 2003; Nameki et al., 2005). Thus, C34 appears to be a suitable peptide to employ in the rational design of an improved HIV fusion inhibitor, based on the interaction between the peptide and the target.

It has been reported that α-helicity of the C-HR and N-HR peptide complexes correlates with the anti-HIV-1 activity of the peptide inhibitor (Chan et al., 1998), suggesting that enhancement of α-helicity of C34 may provide higher affinity to the N-HR region, thus resulting in more potent anti-HIV-1 activity. To design potent fusion inhibitors using the enhancement of α-helicity approach, we divided the α-helical peptide C34 into two characteristic interactive (a, d, e) and solvent accessible (b, c, f, g) sites according to the reported N36/C34 structure (Fig. 1) (Chan et al., 1997). When HIV-1 gp41 is folded, a tryptophan-rich domain (WRD) in the N-terminus of C-HR plays an important role in tight and specific binding, through the interaction of the hydrophobic aromatic ring with a deep groove formed by the N-HR coiled coil (Chan and Kim, 1998; Salzwedel et al., 1999). In fact, C34 contains the N-terminal WRD, which binds to a hydrophobic pocket formed by the amino acid residues L57, W60 and K63 on the N-HR trimer surface (Chan et al., 1998; Ferrer et al., 1999), resulting in higher anti-HIV-1 activity of C34 compared to T-20, which lacks the N-terminal WRD. On the other hand, the solvent accessible site appears to contribute little to the formation of the 6-helix bundles, as demonstrated by the crystal structure of C34 bound to N36 (Chan et al., 1997). Therefore, amino acids in the interactive site are indispensable for binding, whereas those in the solvent accessible site may be replaceable (Fig. 1). To enhance the α-helicity of C34, we introduced a series of systematic replacements of amino acid residues in the solvent accessible site, where the original amino acid residues were substituted with charged and hydrophilic glutamic acid (E) or lysine (K) with the intention of forming possible intrahelical salt-bridges (Marqusee and Baldwin, 1987) (Fig. 1b). We obtained two peptides, SC34 and SC34EK (Fig. 2a), both of which gratifyingly demonstrated increased anti-HIV-1 activity (Otaka et al., 2002).

In this study, we demonstrate that SC34EK maintains highly potent activity against T-20 resistant clones of HIV-1, as well as several clinical isolates, and we reveal that the enhanced α-helicity of SC34EK is indeed involved in the improvement of activity. The activities are specific to HIV-1 and are not influenced by serum components. Structural analysis indicates that electrostatic interactions introduced by EK substitutions enhance the conformational stability of the 6-helix bundle, thus preventing HIV-1 fusion with the host cell. The information from our investigations involving the enhanced α-helicity of SC34EK should enable further design of highly effective and specific HIV-1 inhibitors.

2. Materials and methods

2.1. Cells and viruses

MT-2 and 293T cells were grown in RPMI1640- and Dulbecco's modified Eagle medium (DMEM)-based culture medium, respec-

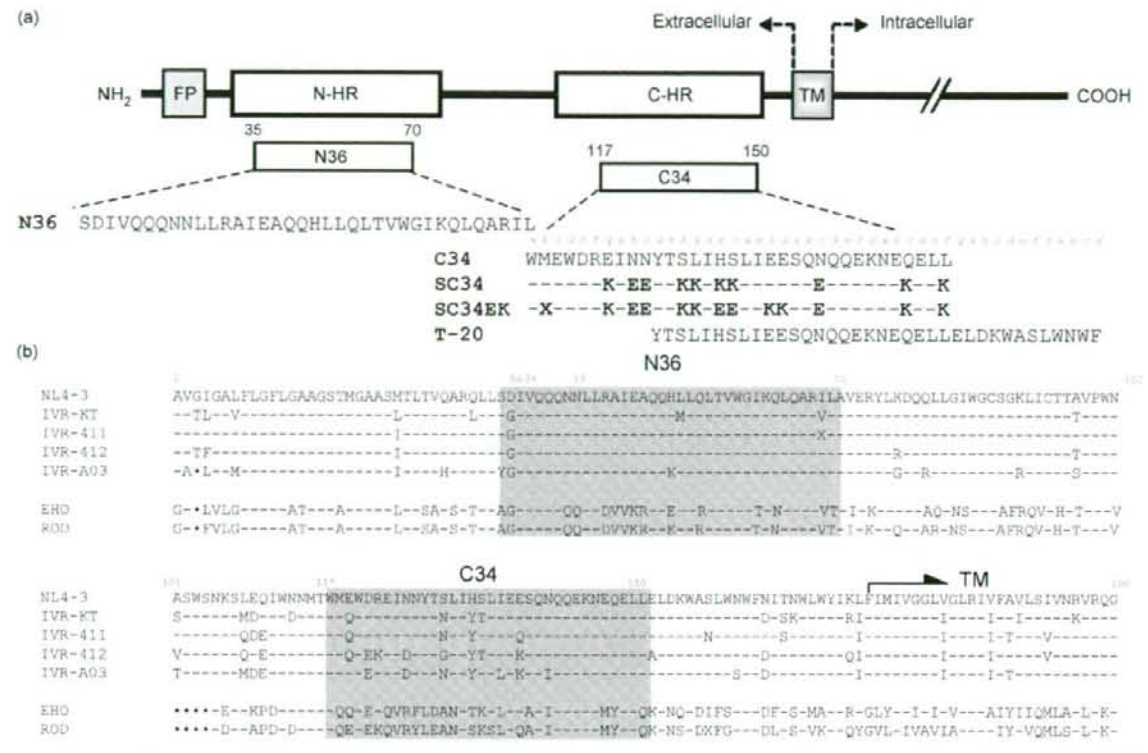

Fig. 2. Schematic view of gp41 and C34 derivatives and amino acid alignment of gp41. (a) The locations of the fusion peptide (FP), the amino-terminal heptad repeat region (N-HR), the carboxyl-terminal heptad repeat region (C-HR), and the transmembrane domain (TM) and the amino acid sequences of N36, T-20, C34 and its derivatives are shown. The residue numbers of each peptide correspond to their positions in gp41 of the NL4-3 strain. The X in SC34EK indicates norleucine, introduced to avoid oxidation of the methionine residues. No differences between the original methionine- and norleucine-containing peptide were observed (Otaka et al., 2002). (b) Alignment of amino acid sequence of clinical isolates (KT, IVR411, IVR412 and IVR-A03; GenBank accession number; AB222704, AB222705, AB222706 and AB222703, respectively) and HIV-2 strains (EHO and ROD) are shown. Corresponding regions of N36 and C34 are indicated in gray. Identical or deleted amino acids from the sequence of NL4-3 are indicated with a bar or a dot, respectively. The X in amino acid sequences of IVR411 and ROD indicates the mixture of I and V for IVR411, and mixture of I and M for ROD.

tively. HeLa-CD4-LTR-β-gal cells were kindly provided by Dr. M. Emerman through the AIDS Research and Reference Reagent Program, Division of AIDS, National Institute of Allergy and Infectious Disease (NIAID) (Bethesda, MD) and were used for the drug susceptibility assay (MAGI assay) as described previously (Kimpton and Emerman, 1992; Kodama et al., 2001; Maeda et al., 1998). The activity of test compounds was determined as the concentration that blocked HIV-1 replication by 50% (EC_{50}).

Laboratory HIV-1 (III_B) and HIV-2 (EHO and ROD) strains were used. An HIV-1 infectious clone pNL4-3 was used for constructions and for the production of HIV-1 variants as described (Nameki et al., 2005). A wild-type HIV-1, HIV-1_{WT}, was generated by transfection of pNL4-3 into 293T cells. Clinical isolates obtained from drug-naïve and heavily drug-experienced patients, were kindly provided by Dr. S. Oka (AIDS Clinical Center, International Medical Center of Japan, Tokyo, Japan). Their co-receptor tropisms were determined using NCK45 cells as described previously (Kajiwara et al., 2006).

2.2. Antiviral agent

The peptide-based fusion inhibitors used in this study were synthesized as described previously (Otaka et al., 2002), and the sequences can be identified in Fig. 2a. 3′-Azido-3′-deoxythymidine (AZT) and 2′,3′-dideoxycytidine (ddC) were purchased from Sigma (St. Louis, MO, USA). MKC-442 was provided by Dr. S. Shigeta (Fukushima Medical University, Fukushima, Japan).

2.3. Determination of drug susceptibility of HIV-1

The peptide sensitivity of infectious clones was determined using the MAGI assay with as described previously (Kodama et al., 2001; Maeda et al., 1998). The activity of test compounds was determined as the concentration that blocks HIV-1 replication by 50% (EC_{50}). For clinical isolates, PHA-stimulated peripheral blood mononuclear cells (PBMCs) were used as described previously (Kodama et al., 2001). PBMCs (10^6 cells/ml) were exposed to test compounds and HIV-1, and were cultured in the presence of interleukin 2 for 7 days. Amounts of p24 protein in the supernatants of the cultures were then determined using the commercially available p24 antigen enzyme linked solvent assay kit.

2.4. Construction of recombinant HIV-1 clone

Recombinant infectious HIV-1 clones with substituted V3 regions, pNL-$V3_{ADA}$ and pNL-$V3_{SF162}$ were generated using pNL4-3. The V3 region, corresponding to n.t. 7029–7249 of pNL4-3, was amplified using primers containing appropriate BglII and NheI restriction enzyme cleavage sites for directional cloning into pBS-

Table 1
Antiviral activity of gp41-derived peptides against gp41 and gp120 V3 recombinant virus[a]

Clone	Tropism[b]	EC_{50} (nM)					
		ddC	N36	T-20	C34	SC34	SC34EK
gp41 recombinant virus							
WT[c]		404 ± 196	180 ± 70	35 ± 17	3.2 ± 0.9	1.4 ± 0.7	0.7 ± 0.3
L33S		289 ± 24	39 ± 11	**>1000**	2.9 ± 0.9	1.3 ± 0.1	0.9 ± 0.3
V38A		714 ± 109	407 ± 76	**402 ± 68**	**96 ± 29**	2.0 ± 0.5	1.1 ± 0.6
V38E		291 ± 57	41 ± 14	**>1000**	**492 ± 85**	**37 ± 12**	**4.3 ± 1.3**
N43K		321 ± 8.5	234 ± 63	114 ± 19	**50 ± 9.5**	2.5 ± 0.3	2.7 ± 0.3
N43D		430 ± 42	461 ± 266	**>1000**	**>100**	**9.0 ± 6.6**	1.0 ± 0.8
D36S/V38M		296 ± 88	178 ± 31	42 ± 6.4	7.2 ± 4.0	1.9 ± 0.1	0.8 ± 0.3
V38E/N42S		273 ± 105	227 ± 20	**>1000**	**322 ± 7.5**	**32 ± 3.1**	3.2 ± 1.0
ΔFNSTW/L33S/N43K[d]		276 ± 39	152 ± 31	**>1000**	**248 ± 56**	2.7 ± 0.3	**4.4 ± 0.5**
ΔFNSTW/D36G/I37K/N126K/L204I[d]		246 ± 67	547 ± 7.8	**754 ± 174**	**67 ± 21**	4.6 ± 0.9	2.9 ± 0.8
gp120 V3 recombinant virus							
V3-ADA	R5	362 ± 102	360 ± 91	**289 ± 19**	6.8 ± 3.3	0.7 ± 0.4	2.0 ± 0.2
V3-SF162[e]	R5	995 ± 219	383 ± 9.9	19 ± 2.8	7.8 ± 3.5	0.5 ± 0.2	0.5 ± 0.2
V3-CH1[f]	R5X4	649 ± 4.5	**2207 ± 42**	16 ± 1	5.6 ± 0.1	1.3 ± 0.1	0.7 ± 0.1
V3-CH2[g]	R5	1515 ± 177	192 ± 13	35 ± 32	3.8 ± 0.1	0.4 ± 0	0.9 ± 0.8

[a] Anti-HIV-1 activity was determined using the MAGI assay. All data represent means ± standard deviation obtained from the results of three independent experiments. Bold indicates over 5-fold increase in EC_{50} value compared to HIV-1_{WT}.

[b] The co-receptor tropism was determined using NCK45 cells as described (Kajiwara et al., 2006).

[c] HIV-1_{NL4-3} served as a wild-type virus.

[d] ΔFNSTW is the deletion of five amino acids at position 364–368 in the gp120 V4 region of HIV-1_{NL4-3} (Nameki et al., 2005). Fusion inhibitor resistant variants used have been previously reported (Armand-Ugon et al., 2003; Nameki et al., 2005).

[e] The V3 region of NL4-3 gp120 was replaced with the corresponding region of HIV-1_{SF162}.

[f] HIV-$1_{V3\text{-}CH1}$ has mutations in the gp120 V3 region of primary isolate HIV-1_{KMT}, where GKI is substituted by GEI.

[g] HIV-$1_{V3\text{-}CH2}$ has mutation in the gp120 V3 region of the primary isolate HIV-1_{KMT}, where GKI is substituted by GQI.

$gp120_{WT}$. The resulting amplified V3 region was subjected to BglII and NheI digestion, subcloned into pBS-$gp120_{WT}$ containing the corresponding region in the DNA fragment of EcoRI–NheI (1510 bp containing gp120 V1, V2 and V3, n.t. 5740–7249 of pNL4-3) and subsequently ligated into pNL4-3. pNL-$V3_{CH1}$ and $V3_{CH2}$, CCR5 and dual (CXCR4 and CCR5) tropic molecular clones, were kindly donated by Dr. Y. Maeda, Kumamoto University (Kumamoto, Japan) (Foda et al., 2001; Maeda et al., 2000).

Recombinant infectious HIV-1 clones carrying various mutations in gp120 and/or gp41 were also generated using pNL4-3. Briefly, the desired mutations were introduced using site directed mutagenesis into the region of pSL-$gp41_{WT}$ flanked by the NheI–BamHI restriction enzyme sites (1220 bp containing gp120 V4, V5 and gp41 ectodomain n.t. 7250–8469 of pNL4-3) (Weiner et al., 1994). After restriction enzyme digestion and purification the NheI–BamHI fragments were ligated into pNL4-3, generating a series of molecular clones with the desired mutations.

Each molecular clone was transfected into 293T cells (10^5 cells/6-well culture plate). After 48 h, MT-2 cells (10^6 cells/well) were added and co-cultured with the 293T cells for an additional 24 h. When an extensive cytopathic effect was observed, the supernatants were harvested and stored at −80 °C for further use.

Table 2
Antiviral activity of gp41-derived peptides against clinical isolates[a]

Strain	EC_{50} (nM)				
	AZT	T-20	C34	SC34	SC34EK
NL4-3 (WT)[b]	2.0	36	3.2	0.36	0.4
KT (WT)[b]	2.0	11	0.2	0.1	0.03
IVR411	**7600**	4.1	0.2	3.1	0.04
IVR412	**9060**	23	7.2	**4.8**	0.1
IVR-A03	**1200**	7.0	**17**	**4.1**	0.7

[a] Anti-HIV-1 activity was determined using the amounts of p24 protein in the supernatants of the PHA-stimulated PBMC cultures using commercially available ELISA kit (Kodama et al., 2001). Bold indicates over 5-fold increase in EC_{50} value compared to HIV-1_{WT}.

[b] HIV-1_{NL4-3} and HIV-1_{KT} served as controls.

2.5. Determination of gp41 amino acid sequence

Nucleotide sequences of the clinical isolates were determined using an automated sequencer. Briefly, DNA was extracted from PBMCs infected with the clinical isolates, subjected to nested PCR for the gp41 coding region, and then directly sequenced as described previously (Nameki et al., 2005).

2.6. Measurement of circular dichroism (CD) spectra

N-HR peptides (N36, $N36_{V38A}$ or $N36_{N43D}$) and C-HR peptides (C34 or SC34EK) were incubated at 37 °C for 30 min (the final concentration of both the N-HR peptide and the C-HR peptide were 10 μM in pH 7.4, 12 mM phosphate-buffered solution containing 50 mM NaCl). The wavelength-dependence of molar ellipticity [θ] was monitored at 25 °C as the average of eight scans, and the thermal stability was estimated by monitoring the change in the CD signal at 222 nm in a spectropolarimeter (Model J-710; Jasco, Tokyo, Japan) equipped with a thermoelectric temperature controller. The midpoint of thermal unfolding transition (melting temperature [T_m]) of each complex was determined as described previously (Otaka et al., 2002). The percentages of a-helicity in 6-helix complexes were calculated by comparing the CD signal at 222 nm of N36/C34 or N36/SC34EK complexes in a spectropolarimeter.

2.7. Crystallization, data collection and refinement

Samples for crystallization were prepared by mixing solutions of N36 and SC34EK dissolved in 10 mM sodium acetate buffer at a concentration of 10 mg/mL. The mixture was incubated for 30 min at 37 °C, then was passed through a 22 μm filter. Crystallization was performed by the hanging drop vapor diffusion method at 4 °C. Droplets were prepared of equal amounts (2 μL) of reservoir solution and the peptide solution. Hexagonal prism crystals were obtained under the following conditions: 100 mM sodium acetate buffer (pH 4.0), 200 mM ammonium sulphate, 14% polyethylene glycol monomethyl ether 2000. After screening of

Table 3
Antiviral activity of HIV-1 gp41-derived peptides against HIV-2[a]

HIV-2 strain	EC_{50} (nM)				
	ddC	T-20	C34	SC34	SC34EK
WT[b]	404 ± 196	35 ± 17	3.2 ± 0.9	1.4 ± 0.7	0.7 ± 0.3
$HIV\text{-}2_{EHO}$[c]	925 ± 188	14 ± 3.0 (×0.4)	**639 ± 87 (×200)**	**68 ± 10 (×49)**	**17 ± 1.2 (×24)**
$HIV\text{-}2_{ROD}$[d]	**1808 ± 927**	**176 ± 68 (×5)**	**>1000 (>×313)**	**251 ± 29 (×179)**	**115 ± 33 (×164)**

[a] Anti-HIV-2 activity was determined using the MAGI assay. All data represent mean ± standard deviation obtained from the results of three independent experiments. Bold indicates over 5-fold increase in EC_{50} value compared to $HIV\text{-}1_{WT}$.
[b] $HIV\text{-}1_{NL4\text{-}3}$ served as a wild-type virus.
[c] $HIV\text{-}2_{EHO}$ was dual-tropic HIV-2.
[d] $HIV\text{-}2_{ROD}$ was T-tropic HIV-2.

various cryo-conditions, the suitable condition was found to be the addition of 35% xylitol to the peptide solution and a slight increase in the amount of the precipitant (*ca* 14.5%). The obtained crystals were easily broken by direct transfer from the crystallization condition to the cryo-condition, but the transfer of the fragile crystals could be accomplished by gradual change in conditions using stepwise increase in the amount (0–35% in five steps) of the cryoprotectant.

Data were collected at a beamline BL38B1 of SPring-8. Collected data were processed using DENZO and SCALEPACK from the HKL2000 package (Otwinowski and Minor, 1997). A molecular replacement solution was found using AMoRe (Navaza, 2001), with a molecular model of the HIV-1 gp41 core structure (PDB code: 1AIK). Model refinements and reconstruction were performed using REFMAC5 (Murshudov et al., 1999) and XtalView (McRee, 1999). The final model was refined at a resolution of 2.1 Å, to a crystallographic *R* value of 0.213 and a free *R* value of 0.238. Detailed data collection and refinement statistics are summarized in Table 1. Atomic coordinates and structural factors have been deposited at the Protein Data Bank (PDB code:2Z2T).

3. Results

3.1. Anti-HIV-1 activity of SC34 and SC34EK

We examined the anti-HIV-1 activity of SC34 and SC34EK against not only $HIV\text{-}1_{WT}$ but also T-20- and/or C34-resistant clones observed in vitro. SC34 and especially SC34EK that has aligned EK modification more effectively suppress HIV-1 infection compared to C34 and T-20 (Table 1). D36S/V38M substitutions in the gp41 region ($HIV\text{-}1_{D36S/V38M}$), and a five amino acid (FNSTW) deletion in the V4 region of gp120 (ΔV4) with L33S/N43K in the gp41 region ($HIV\text{-}1_{\Delta V4/L33S/N43K}$) were isolated in vitro (Fikkert et al., 2002; Rimsky et al., 1998). L33S was also selected during C34-resistant induction in vitro (Armand-Ugon et al., 2003). C34 and its derivatives effectively inhibit entry of these clones into the host cell. In particular, SC34EK maintained strong activity even against V38E containing clones, such as $HIV\text{-}1_{V38E/N42S}$ (Armand-Ugon et al., 2003), which showed cross-resistance to T-20, C34 and SC34. Reduction of activities by SC34 and SC34EK was moderate in $HIV\text{-}1_{\Delta FNSTW/L33S/N43K}$ that showed high level resistance to T-20 and C34. Next, we examined the antiviral activities of C34 derivatives against clones containing major primary mutations V38A and N43D, which are mutations frequently observed in T-20 resistant variants in vivo (Cabrera et al., 2006; Derdeyn et al., 2001; Menzo et al., 2004; Poveda et al., 2004; Poveda et al., 2002; Xu et al., 2005) (Table 1). SC34 reduced its antiviral activities against $HIV\text{-}1_{N43D}$, while SC34EK maintained its potent activity, indicating that when EK is bound with the complementary electrostatic interactions appropriately aligned SC34EK can effectively suppress the infection by various clones resistant to T-20 and C34 both in vitro and in vivo.

We further evaluated activities of SC34 and SC34EK against V3-substituted clones (Table 1). $HIV\text{-}1_{V3\text{-}ADA}$ uses mainly the CCR5 co-receptor for its entry into the host cells and has been reported to moderate T-20 resistance (≈10 fold), compared to the CXCR4 using strain of HIV-1, which shows higher susceptibility to fusion inhibitors (Reeves et al., 2002). As reported, the susceptibility of $HIV\text{-}1_{V3\text{-}ADA}$ to T-20 decreased, however, C34 and its derivatives maintained their activity against the same variant. Interestingly, in our experiments, $HIV\text{-}1_{V3\text{-}SF162}$, $HIV\text{-}1_{V3\text{-}CH1}$ and $HIV\text{-}1_{V3\text{-}CH2}$ also showed comparable susceptibility to T-20. These results indicate that sequence variations in the V3 region do not always correlate with the observed T-20 susceptibility and are not involved in the resistance to C34 and its derivatives.

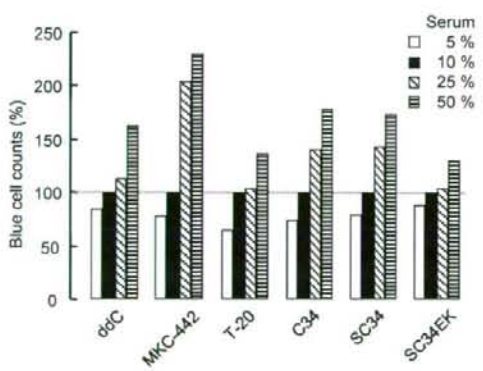

Fig. 3. Effect of FCS concentrations on anti-HIV-1 activity. Changes in the blue cell counts at various concentrations of FCS are shown. Blue cell counts at EC_{80} value in 10% FCS concentration (black bar) were used and set as 100%. White, black, hatched, and striped bars correspond to 5, 10, 25, and 50% FCS, respectively. Inhibitors for reverse transcriptase, ddC and MKC-442, and for fusion, T-20 were used as controls.

3.2. Amino acid sequence

Amino acid sequences of clinical isolates are shown in Fig. 2b. One isolate, $HIV\text{-}1_{KT}$, was obtained from a drug-naïve patient and the other three isolates ($HIV\text{-}1_{411}$, $HIV\text{-}1_{412}$, $HIV\text{-}1_{A03}$) were obtained from heavily drug-experienced patients. None of the patients had received T-20 therapy. Amino acid sequences of the N-HR were highly conserved within all HIV-1 clinical isolates with some small variations. In contrast, the N36 region of the two HIV-2 strains, EHO and ROD, was identical in both HIV-2 isolates. We found some variations in the amino acid sequences of the HIV-2 strains we isolated, as compared with the sequences deposited in the GenBank (accession number; M15390 and X05291 for $HIV\text{-}2_{ROD}$, and U272000 for $HIV\text{-}2_{EHO}$). Namely, we identified two different amino acids in the isolated $HIV\text{-}2_{ROD}$, V26L and

I157I/M (mixture of I and M), and one variation in the amino acid sequence of HIV-2_{EHO}. V45L. Except for I157M, other substitutions are observed in the majority of the HIV-2 strains, as reported in the HIV sequence database (Los Alamos National Laboratory: Los Alamos, NM, USA, http://www.hiv.lanl.gov). These substitutions might be introduced through different culture conditions, (e.g., host cells used for the propagation). We considered these substitutions as a polymorphism.

Sequence homology of the N36 region of the isolated HIV-1 strains was 31/36 (86%), including mutation D36G that is observed in the vast majority of HIV-1 strains (Kuiken et al., 2001). In contrast, those of the C34 region were relatively heterogeneous, 24/34 (71%) for HIV-1 and 12/34 (35%) for HIV-2. Sequence identity of the T-20 region (residues 117–152) in the HIV-1 strains was also variable 27/36 (75%), while in the HIV-2 strains the sequence identity was 15/36 (42%). These results indicate that even highly conserved two helical extracellular domain of the gp41 can allow polymorphisms.

3.3. Efficacy of the peptides against clinical isolates

To evaluate preclinical efficacy, we examined the antiviral activity of C34, SC34 and SC34EK against clinical isolates (Table 2). Replication of HIV-1_{NL4-3} and HIV-1_{KT}, a drug-naïve strain, was suppressed by all compounds tested. C34 showed decreased activity against HIV-$1_{IVR-A03}$, which was isolated from a heavily drug-exposed patient. SC34 also showed reduced susceptibility against three drug-experienced strains. However, it is difficult to conclude whether SC34 showed enhanced susceptibility against HIV-1_{KT} or reduced susceptibility against drug resistant strains. In contrast, T-20 and SC34EK suppressed the replication of all isolates tested to similar extents in EC_{50} values compared to HIV-1_{NL4-3} (Table 2), indicating that SC34EK with appropriately aligned EK residues effectively suppresses the replication of the clinical 3 isolates.

3.4. Anti-HIV-2 activity

To confirm the target specificity, we examined antiviral activities of SC34 and SC34EK against two HIV-2 strains, EHO and ROD. Compared to HIV-1_{NL4-3}, EHO and ROD contain 19 and 22 amino acid substitutions in the C34 region, respectively, and 15 amino acid substitutions in the N36 region, the anticipated site of binding of SC34 and SC34EK peptides (Fig. 2b). Like the parent peptide C34, both SC34 and SC34EK lost their potent activities (Table 3). Compared to HIV-1_{NL4-3}, 6 out of 19 residues in the C34 region of HIV-2_{EHO} and 7 out of 22 residues in the C34 region of HIV-2_{ROD} are located at positions *a*, *d*, and *e* that directly interact with the N36 binding surface. These substitutions in the N36 and C34 region in HIV-2 may be responsible for reduced anti-HIV-2 activities of the peptides derived from HIV-1. At present, we cannot conclude which amino acid substitutions are directly involved in the reduced susceptibility of the HIV-2 strain to the treatment with the peptide fusion inhibitor, and/or whether other regions besides the N36 and C34 regions might influence peptide susceptibility. However, our results indicate that SC34 and SC34EK maintain similar target specificity to the parent peptide, C34.

3.5. Effect of fetal calf serum (FCS) on anti-HIV-1 activity

To estimate the stability of the peptides in vivo, binding level of SC34EK, to serum components, (e.g., albumin) was examined. In this experiment, the antiviral activity in the presence of relatively high concentrations of fetal calf serum (FCS) was determined (Baba et al., 1993) (Fig. 3). EC_{80} values of the fusion inhibitors against HIV-1 replication in vitro were used. In the presence of 50% FCS, the activity of MKC-442 (I-EBU), a lipophilic non-nucleoside RT inhibitor, was reduced 2.3-fold compared with 10% FCS as described previously (Baba et al., 1993). However, the activities of SC34, SC34EK and T-20 were little influenced by serum components. Among the three, SC34EK was the least affected by the concentration of FCS.

We further examined the stability of peptide inhibitors in freshly prepared human sera ($n = 3$). After 1 h incubation of peptides in human sera (final concentration of 200 μM) at 37 °C, the anti-HIV-1 activity was examined using the MAGI assay. Comparable activities of all peptides tested were observed either with or without the incubation (data not shown). These results indicate that hydrophilic SC34EK likely retains its strong anti-HIV-1 activity in vivo, similarly to T-20, because of its low non-specific binding and protease cleavage in serum.

3.6. Peptide binding affinity

To clarify the mechanism of potent anti-HIV-1 activity observed with SC34EK, the binding affinity of SC34EK was evaluated by collecting the CD spectra using synthetic peptides. The CD spectra of equimolar mixtures of the N-HR and C-HR peptides showed spectrum minima at 208 and 222 nm, which indicate the presence of stable α-helical conformations. All combinations of peptides showed similar spectra at 25 °C, indicating that these peptides contained the same α-helicity (Fig. 4a), although the spectrum of C34 with N36 and N43D mutation ($N36_{N43D}$) indicated only weak α-helicity. These results indicate that N43D might reduce the stability of the conformation of the 6-helix bundle, thus decreasing the replication of HIV-1, whereas V38A does not. SC34EK formed stable 6-helix conformations with $N36_{V38A}$ and $N36_{N43D}$. Under these experimental conditions, wavelength-dependent spectra were similar with the exception of the spectrum of the $N36_{N43D}$/C34 complex. Thus, we analyzed thermal stabilities, defined as the midpoint of the thermal unfolding transition (T_m) values, of the potential 6-helix bundles of N-HR and C-HR peptides. T_m of N36/C34 was found to be 52.0 °C, while that of $N36_{V38A}$/C34 and $N36_{N43D}$/C34 decreased to 44.5 and 34.0 °C, respectively (Fig. 3b). In contrast, thermal stabilities of $N36_{V38A}$/SC34EK, $N36_{N43D}$/SC34EK and N36/SC34EK were much higher, 60.5, 56.0 and 69.5 °C, respectively. Thus, binding affinity of SC34EK to N-HR was stronger compared to that of C34. Alternatively, at the physiological temperature of 37 °C, only 60 and 40% of the α-helix content was observed in $N36_{V38A}$/C34 and $N36_{N43D}$/C34 mixtures, respectively, indicating that roughly half of C34 failed to form stably 6-helix bundle with the target N-HR harboring resistant mutations. Therefore, C34 reduces its anti-fusion activity exerted by dominant negative effect. In contrast, only 20% of the unfolded α-helix content was observed in SC34EK with mutated N36, which indicated that at 37 °C, binding of SC34EK to mutated N36 was comparable to that of C34 with wild-type N36 (Fig. 4b). Moreover, physiochemical properties of N-HR and SC34EK complexes, defined by T_m value, correlated well with their ability to inhibit HIV-1 fusion (Fig. 4c). These results suggest that the stability of the 6-helix complex, as judged by the binding stability (affinity), is directly correlated with the anti-HIV-1 activity.

3.7. Crystal structure of the N36/SC34EK complex

The crystal structure of the complex between SC34EK and the N-HR representative peptide N36 was resolved to a resolution of 2.1 Å (Table 4). In the asymmetric unit, a 6-helix bundle consisting of a central helix bundle of three N36 peptides surrounded by three SC34EK peptides was found. This arrangement is similar in the core structure of gp41 (Chan et al., 1997). Structural superimposition of the original gp41 core and the N36/SC34EK complex showed a good match, with an RMSD value of 0.59 for main-chain atoms

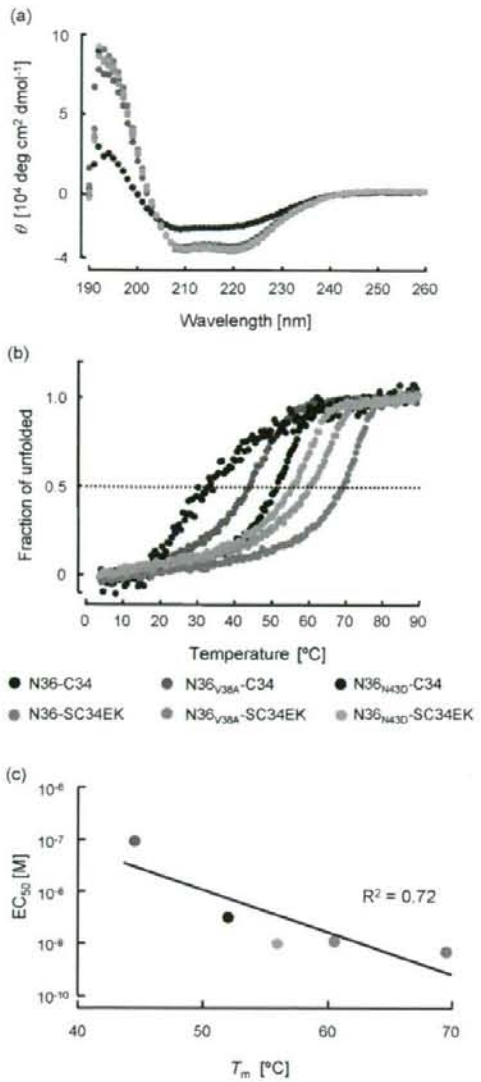

Fig. 4. CD analysis of peptide complex between resistant variants of N36 and C34 or SC34EK. (a) Wavelength-dependent CD spectra of the complexes in solution. The spectrum minima at 208 and 222 nm indicated the presence of stable α-helical conformations. (b) Thermal midpoint analysis was measured at 222 nm CD signal for the N and C peptide complexes. Final concentration of each peptide was 10 mM. The arrow indicates the physiological temperature of 37 °C. (c) The correlation between T_m (b) and EC_{50} values (Table 1). Colors of plots correspond to those in panels (a) and (b). Combination of $N36_{N43D}$ and C34 (EC_{50} > 100 nM) is excluded.

(Fig. 5a and b). Hydrophobic contacts between SC34EK and N36 with tryptophan rich domain (WRD) and leucine zipper were preserved for the original gp41 core. All introduced charged residues of the EK motif were directed toward the solvent (Fig. 5c). As a direct consequence of introducing the EK motifs, the ratio of surface area occupied by charged residues to the total surface area was increased from 35% in the original molecule to 60% in the N36/SC34EK complex. Importantly, it appeared that tight bonding, such as ion pairing or hydrogen bonding, was not present in the

Table 4
Crystallization, data collection and refinement statistics

Data collection	BL38B1 Spring-8
Temperature (K)	100
Space group	$P3_121$
Cell dimensions *a*, *b*, *c* (Å)	105.01, 105.01, 78.31
Resolution limits (Å)	90.00–2.10
Number of unique reflections	29,461
Average redundancy	7.53
Completeness (%)	99.7
R_{merge} [a]	0.122
Refinement statistics	
Refinements resolution range (Å)	20.00–2.20
R/R_{free} [b] (%)	0.213/0.238
The highest resolution shell (Å)	2.15–2.10
R/R_{free} [b] (%)	0.231/0.255
RMSD from ideal	
Bonds (Å)	0.010
Angles (°)	1.015
⟨*B*⟩ for atomic model[c] (Å²)	29.93
Ramachandran plot	
Most favored regions (%)	100

[a] $R_{merge} = \sum|I_h - \langle I_h\rangle| / \sum I_h$, where $\langle I_h\rangle$ is the average intensity of reflection *h* and symmetry-related reflections.

[b] *R* and $R_{free} = \sum||F_o| - |F_c|| / \sum|F_o|$ calculated for reflections of the working set and test (5%) set, respectively.

[c] ⟨*B*⟩ is the average temperature factor for all protein atoms.

side-chains of the residues of the EK motif. Electrostatic interaction may involve in constrained structure which provides the enhanced α-helicity observed (Fig. 4). This structural analysis demonstrated that the interaction between N36 and SC34EK retained the ability to form the 6-helix bundle structure despite the substitution of more than one third of the residues (13/34) in the sequence of SC34EK.

4. Discussion

In this study, we characterized a novel α-helical peptide, SC34EK that effectively inhibits replication of HIV-1 strains resistant to T-20 and C34. The activity was specific to HIV-1 and little influenced by serum components. We demonstrate that the potent anti-HIV-1 activity of SC34EK is derived from its high affinity to the N-HR region by the CD analysis. Further, we reveal that SC34EK binds to its target, N-HR in identical manner that C34 does by the structure analysis.

The structural analysis of the N36/SC34EK complex clearly demonstrated that the interaction between SC34EK and N36 peptides was maintained by hydrophobic contacts and that the EK motif was directed toward the solvent. The introduction of the EK residues increased the proportion of accessible surface area occupied by charged residues. Although tight bonding was not observed, a continuous electrostatic potential between the EK residues may serve to stabilize the helix bundle. Such helix stabilization, which might occur on the surface of the HIV-1 virion between SC34EK and the N36 region of gp41, could result in the high anti-HIV-1 activity. In this regard, SC34EK, containing an aligned EK motif, showed more potent anti-HIV-1 activity compared to SC34, which has one misaligned EK motif (Fig. 2a). Increasing the hydrophilic surface area may prevent aggregation of SC34EK as compared to parental peptide C34. Therefore, SC34EK might distribute into the various organs in the body without being trapped and destroyed in the reticular systems or having its activity reduced by non-specific binding to proteins (e.g., albumin) (Fig. 3).

We further demonstrate that SC34EK specifically binds to the target, N-HR of HIV-1, since it only exerted weak activity to two

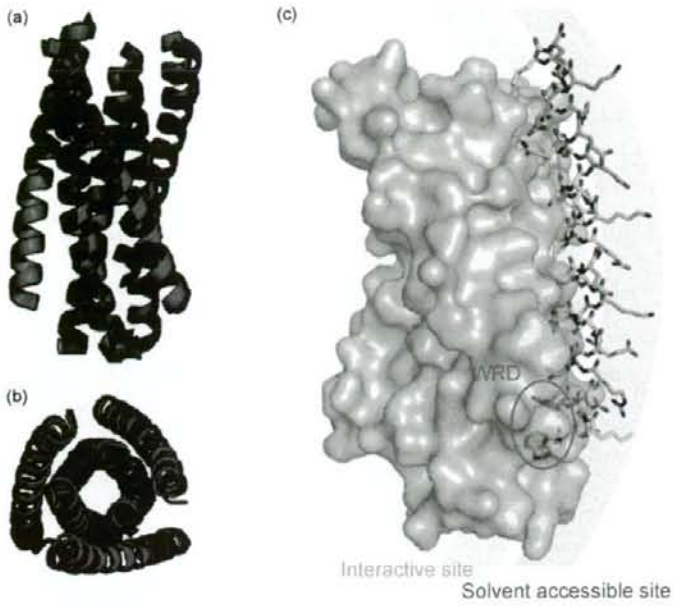

Fig. 5. Structure of the 6-helix bundle formed by N36 and SC34EK. (a and b) The gp41 core structure and N36/SC34EK complex are shown in red and blue, respectively. (c) Stick model representation of SC34EK. The stick model of SC34EK is shown, and three N36s in the core and two other surrounded SC34EK are represented in gray. SC34EK showed amphiphilic properties. The location of the N-terminal tryptophan rich domain (WRD) in SC34EK is indicated by a red circle. Original and introduced charged amino acids are indicated in green and blue, respectively.

HIV-2 strains that contain 15 amino acid substitutions in the N-HR compared to HIV-1 NL4-3 strain (Table 3 and Fig. 2b). These results suggest that to develop resistance to SC34EK, at least, certain mutations in not only the N-HR but also the C-HR are required to be introduced. This might delay emergence of resistant HIV-1 variants to SC34EK in vivo.

So far, some approaches for stabilizing α-helix structures through the introduction of artificial amino acids were reported for HIV-1 fusion inhibitors T-20 (Judice et al., 1997) and C34 (Sia et al., 2002), including an example of an amino acid containing terminal olefin-derived side chains, designed as a substrate for the ring-closing olefin metathesis (Blackwell et al., 2001) and an example of a hydrocarbon-stapled peptides (Phelan et al., 1997) Walensky et al. (2004) applied a hydrocarbon-stapled modification to generate peptides that bind to the BH3 helical domain of Bcl-2, an anti-apoptotic protein, and demonstrated that a synthesized peptide mimic that binds to the BH3 domain activates apoptosis in leukemic cells. However, all peptides exerted only moderate activity in vivo, although they showed efficient binding to the target proteins in vitro (Blackwell et al., 2001; Judice et al., 1997; Sia et al., 2002; Walensky et al., 2004). It is likely that during the formation of the 6-helix bundle and the fusion process, gp41 changes its conformation drastically, suggesting that a flexible conformation of the peptide may be required to preserve actual inhibition. Compared with tethered, constrained peptides, EK modification that facilitates electrostatic stabilization displays such flexibility while exhibiting enhanced α-helicity. Most recently, T290676, a 38 amino acid peptide, has been reported to suppress various fusion inhibitor-resistant strains of HIV-1 (Dwyer et al., 2007). Like SC34EK, T290676 is substituted with the charged and hydrophilic amino acids, glutamic acid (E) and arginine (R), at the solvent accessible site and shows potent anti-HIV-1 activity.

In conclusion, we have demonstrated that SC34EK selectively inhibits various HIV-1 strains, including T-20 resistant clones, through increased stability of the α-helix. The sequence of the solvent accessible site of α-helical peptides is replaceable and modifications of this sequence can regulate α-helicity with target specificity. Therefore, our approach of introducing the EK motif in the α-helical structure of the peptide inhibitor will help to generate future peptide inhibitors with high anti-HIV efficacy and potentially fewer adverse effects.

Acknowledgements

This work was supported in part by grants for the Promotion of AIDS Research from the Ministry of Health and Welfare and for the Ministry of Education, Culture, Sports, Science, and Technology (MEXT) of Japan (E.K. and S.O.); a grant for Research for Health Sciences Focusing on Drug Innovation from the Japan Health Sciences Foundation (E.K., S.O., N.F. and M.M.), the Program of Founding Research Centers for Emerging and Reemerging Infectious Diseases by the MEXT (S.N.), a Health and Labor Sciences Research Grant for Research on HIV/AIDS from the Ministry of Health and Labor of Japan (S.N.), and the 21st Century COE program (H.N., K.K., K.I. and N.F.). H.N. is grateful for the JSPS Research Fellowships for Young Scientists. Appreciation is expressed to Mr. Maxwell Reback (Kyoto University) for reading this manuscript.

References

Aquaro S, D'Arrigo R, Svicher V, Perri GD, Caputo SL, Visco-Comandini U, et al. Specific mutations in HIV-1 gp41 are associated with immunological success in HIV-1-infected patients receiving enfuvirtide treatment. J Antimicrob Chemother 2006;58:714–22.

Armand-Ugon M, Gutierrez A, Clotet B, Este JA. HIV-1 resistance to the gp41-dependent fusion inhibitor C-34. Antiviral Res 2003;59:137–42.

Baba M, Yuasa S, Niwa T, Yamamoto M, Yabuuchi S, Takashima H, et al. Effect of human serum on the in vitro anti-HIV-1 activity of 1-[(2-hydroxyethoxy)methyl]-6-(phenylthio)thymine (HEPT) derivatives as related to their lipophilicity and serum protein binding. Biochem Pharmacol 1993;45:2507–12.
Baldwin CE, Berkhout B. Second site escape of a T20-dependent HIV-1 variant by a single amino acid change in the CD4 binding region of the envelope glycoprotein. Retrovirology 2006;3:84.
Blackwell HE, Sadowsky JD, Howard RJ, Sampson JN, Chao JA, Steinmetz WE, et al. Ring-closing metathesis of olefinic peptides: design, synthesis, and structural characterization of macrocyclic helical peptides. J Org Chem 2001;66:5291–302.
Cabrera C, Marfil S, Garcia E, Martinez-Picado J, Bonjoch A, Bofill M, et al. Genetic evolution of gp41 reveals a highly exclusive relationship between codons 36, 38 and 43 in gp41 under long-term enfuvirtide-containing salvage regimen. AIDS 2006;20:2075–80.
Chan DC, Chutkowski CT, Kim PS. Evidence that a prominent cavity in the coiled coil of HIV type 1 gp41 is an attractive drug target. Proc Natl Acad Sci U S A 1998;95:15613–7.
Chan DC, Fass D, Berger JM, Kim PS. Core structure of gp41 from the HIV envelope glycoprotein. Cell 1997;89:263–73.
Chan DC, Kim PS. HIV entry and its inhibition. Cell 1998;93:681–4.
Derdeyn CA, Decker JM, Sfakianos JN, Wu X, O'Brien WA, Ratner L, et al. Sensitivity of human immunodeficiency virus type 1 to the fusion inhibitor T-20 is modulated by coreceptor specificity defined by the V3 loop of gp120. J Virol 2000;74:8358–67.
Derdeyn CA, Decker JM, Sfakianos JN, Zhang Z, O'Brien WA, Ratner L, et al. Sensitivity of human immunodeficiency virus type 1 to fusion inhibitors targeted to the gp41 first heptad repeat involves distinct regions of gp41 and is consistently modulated by gp120 interactions with the coreceptor. J Virol 2001;75:8605–14.
Dwyer JJ, Wilson KL, Davison DK, Freel SA, Seedorff JE, Wring SA, et al. Design of helical, oligomeric HIV-1 fusion inhibitor peptides with potent activity against enfuvirtide-resistant virus. Proc Natl Acad Sci U S A 2007;104:12772–7.
Ferrer M, Kapoor TM, Strassmaier T, Weissenhorn W, Skehel JJ, Oprian D, et al. Selection of gp41-mediated HIV-1 cell entry inhibitors from biased combinatorial libraries of non-natural binding elements. Nat Struct Biol 1999;6:953–60.
Fikkert V, Cherepanov P, Van Laethem K, Hantson A, Van Remoortel B, Pannecouque C, et al. env chimeric virus technology for evaluating human immunodeficiency virus susceptibility to entry inhibitors. Antimicrob Agents Chemother 2002;46:3954–62.
Foda M, Harada S, Maeda Y. Role of V3 independent domains on a dual-tropic human immunodeficiency virus type 1 (HIV-1) envelope gp120 in CCR5 coreceptor utilization and viral infectivity. Microbiol Immunol 2001;45:521–30.
Judice JK, Tom JY, Huang W, Wrin T, Vennari J, Petropoulos CJ, et al. Inhibition of HIV type 1 infectivity by constrained alpha-helical peptides: implications for the viral fusion mechanism. Proc Natl Acad Sci U S A 1997;94:13426–30.
Kajiwara K, Kodama E, Matsuoka M. A novel colorimetric assay for CXCR4 and CCR5 tropic human immunodeficiency viruses. Antivir Chem Chemother 2006;17:215–23.
Kimpton J, Emerman M. Detection of replication-competent and pseudotyped human immunodeficiency virus with a sensitive cell line on the basis of activation of an integrated beta-galactosidase gene. J Virol 1992;66:2232–9.
Kodama EI, Kohgo S, Kitano K, Machida H, Gatanaga H, Shigeta S, et al. 4′-Ethynyl nucleoside analogs: potent inhibitors of multidrug-resistant human immunodeficiency virus variants in vitro. Antimicrob Agents Chemother 2001;45:1539–46.
Kuiken C, Foly B, Hahn B, Marx P, McCutchan F, Mellors J, et al.Kuiken C, Foly B, Hahn B, Marx P, McCutchan F, Mellors J, Wolinsky S, Korber B, editors. HIV Sequence Compendium 2001. Los Alamos, NM: Los Alamos National Laboratory; 2001.
Lalezari JP, Henry K, O'Hearn M, Montaner JS, Piliero PJ, Trottier B, et al. Enfuvirtide, an HIV-1 fusion inhibitor, for drug-resistant HIV infection in North and South America. N Engl J Med 2003;348:2175–85.
Lazzarin A, Clotet B, Cooper D, Reynes J, Arasteh K, Nelson M, et al. Efficacy of enfuvirtide in patients infected with drug-resistant HIV-1 in Europe and Australia. N Engl J Med 2003;348:2186–95.
Liu S, Lu H, Niu J, Xu Y, Wu S, Jiang S. Different from the HIV fusion inhibitor C34, the anti-HIV drug fuzeon (T-20) inhibits HIV-1 entry by targeting multiple sites in gp41 and gp120. J Biol Chem 2005;280:11259–73.
Maeda Y, Foda M, Matsushita S, Harada S. Involvement of both the V2 and V3 regions of the CCR5-tropic human immunodeficiency virus type 1 envelope in reduced sensitivity to macrophage inflammatory protein 1alpha. J Virol 2000;74:1787–93.
Maeda Y, Venzon DJ, Mitsuya H. Altered drug sensitivity, fitness, and evolution of human immunodeficiency virus type 1 with pol gene mutations conferring multi-dideoxynucleoside resistance. J Infect Dis 1998;177:1207–13.
Marqusee S, Baldwin RL. Helix stabilization by Glu-.Lys+ salt bridges in short peptides of de novo design. Proc Natl Acad Sci U S A 1987;84:8898–902.
Matthews T, Salgo M, Greenberg M, Chung J, DeMasi R, Bolognesi D. Enfuvirtide: the first therapy to inhibit the entry of HIV-1 into host CD4 lymphocyte. Nat Rev Drug Discov 2004;3:215–25.
McRee DE. XtalView/Xfit—a versatile program for manipulating atomic coordinates and electron density. J Struct Biol 1999;125:156–65.
Menzo S, Castagna A, Monachetti A, Hasson H, Danise A, Carini E, et al. Genotype and phenotype patterns of human immunodeficiency virus type 1 resistance to enfuvirtide during long-term treatment. Antimicrob Agents Chemother 2004;48:3253–9.
Mink M, Mosier SM, Janumpalli S, Davison D, Jin L, Melby T, et al. Impact of human immunodeficiency virus type 1 gp41 amino acid substitutions selected during enfuvirtide treatment on gp41 binding and antiviral potency of enfuvirtide in vitro. J Virol 2005;79:12447–54.
Murshudov GN, Vagin AA, Lebedev A, Wilson KS, Dodson EJ. Efficient anisotropic refinement of macromolecular structures using FFT. Acta Crystallogr 1999;D55:247–55.
Nameki D, Kodama E, Ikeuchi M, Mabuchi N, Otaka A, Tamamura H, et al. Mutations conferring resistance to human immunodeficiency virus type 1 fusion inhibitors are restricted by gp41 and Rev-responsive element functions. J Virol 2005;79:764–70.
Navaza J. Implementation of molecular replacement in AMoRe. Acta Crystallogr 2001;D57(Pt 10):1367–72.
Otaka A, Nakamura M, Nameki D, Kodama E, Uchiyama S, Nakamura S, et al. Remodeling of gp41-C34 peptide leads to highly effective inhibitors of the fusion of HIV-1 with target cells. Angew Chem Int Ed Engl 2002;41:2937–40.
Otwinowski Z, Minor W. Processing of X-ray diffraction data collected in oscillation mode. Met Enzymol 1997;276:307–26.
Phelan JC, Skelton NJ, Braisted AC, McDowell RS. A general method for constraining short peptides to an alpha-helical conformation. J Am Chem Soc 1997;119:455–60.
Poveda E, Rodes B, Labernardiere JL, Benito JM, Toro C, Gonzalez-Lahoz J, et al. Evolution of genotypic and phenotypic resistance to Enfuvirtide in HIV-infected patients experiencing prolonged virologic failure. J Med Virol 2004;74:21–8.
Poveda E, Rodes B, Toro C, Martin-Carbonero L, Gonzalez-Lahoz J, Soriano V. Evolution of the gp41 env region in HIV-infected patients receiving T-20, a fusion inhibitor. AIDS 2002;16:1959–61.
Reeves JD, Gallo SA, Ahmad N, Miamidian JL, Harvey PE, Sharron M, et al. Sensitivity of HIV-1 to entry inhibitors correlates with envelope/coreceptor affinity, receptor density, and fusion kinetics. Proc Natl Acad Sci U S A 2002;99:16249–54.
Rimsky LT, Shugars DC, Matthews TJ. Determinants of human immunodeficiency virus type 1 resistance to gp41-derived inhibitory peptides. J Virol 1998;72:986–93.
Salzwedel K, West JT, Hunter E. A conserved tryptophan-rich motif in the membrane-proximal region of the human immunodeficiency virus type 1 gp41 ectodomain is important for Env-mediated fusion and virus infectivity. J Virol 1999;73:2469–80.
Sia SK, Carr PA, Cochran AG, Malashkevich VN, Kim PS. Short constrained peptides that inhibit HIV-1 entry. Proc Natl Acad Sci U S A 2002;99:14664–9.
Walensky LD, Kung AL, Escher I, Malia TJ, Barbuto S, Wright RD, et al. Activation of apoptosis in vivo by a hydrocarbon-stapled BH3 helix. Science 2004;305:1466–70.
Wei X, Decker JM, Liu H, Zhang Z, Arani RB, Kilby JM, et al. Emergence of resistant human immunodeficiency virus type 1 in patients receiving fusion inhibitor (T-20) monotherapy. Antimicrob Agents Chemother 2002;46:1896–905.
Weiner MP, Costa GL, Schoettlin W, Cline J, Mathur E, Bauer JC. Site-directed mutagenesis of double-stranded DNA by the polymerase chain reaction. Gene 1994;151:119–23.
Wild C, Oas T, McDanal C, Bolognesi D, Matthews T. A synthetic peptide inhibitor of human immunodeficiency virus replication: correlation between solution structure and viral inhibition. Proc Natl Acad Sci U S A 1992;89:10537–41.
Xu L, Pozniak A, Wildfire A, Stanfield-Oakley SA, Mosier SM, Ratcliffe D, et al. Emergence and evolution of enfuvirtide resistance following long-term therapy involves heptad repeat 2 mutations within gp41. Antimicrob Agents Chemother 2005;49:1113–9.
Xu Y, Hixon MS, Dawson PE, Janda KD. Development of a FRET assay for monitoring of HIV gp41 core disruption. J Org Chem 2007;72:6700–7.